Landes Bioscience www.landesbioscience.com

Supplemental Material to:

Rui Liu, Jingyi Li, Tao Zhang, Linzhi Zou, Yi Chen, Kui Wang, Yunlong Lei, Kefei Yuan, Yi Li, Jiang Lan, Lin Cheng, Na Xie, Rong Xiang, Edouard C Nice, Canhua Huang, and YuquanWei

Itraconazole suppresses the growth of glioblastoma through induction of autophagy: Involvement of abnormal cholesterol trafficking

Autophagy 2014; 10(7)
http://dx.doi.org/10.4161/auto.28912

www.landesbioscience.com/journals/autophagy/article/28912

Figure S1

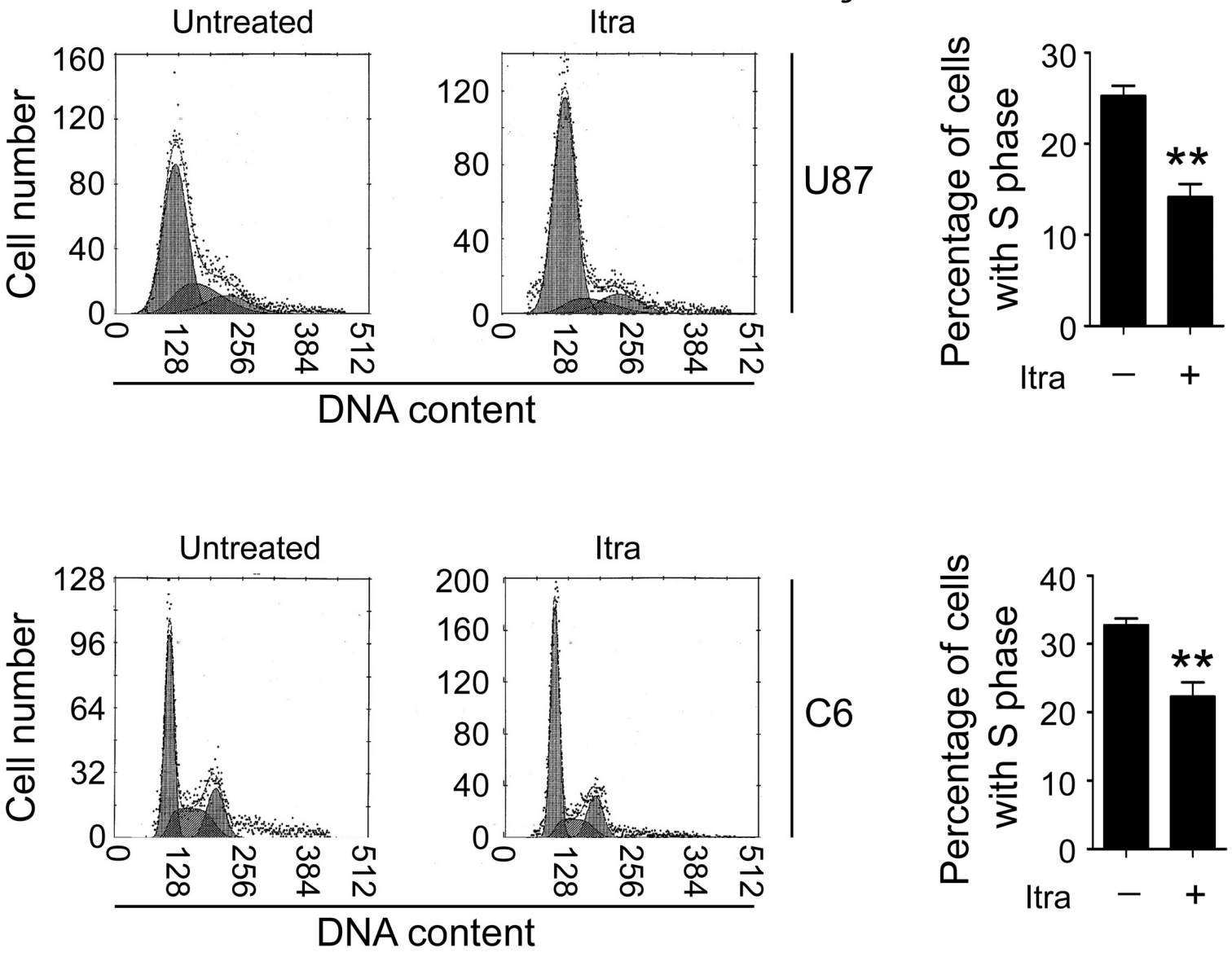
Untreated
Itra
Cell number
DNA content
U87
C6
Percentage of cells with S phase
Itra
**

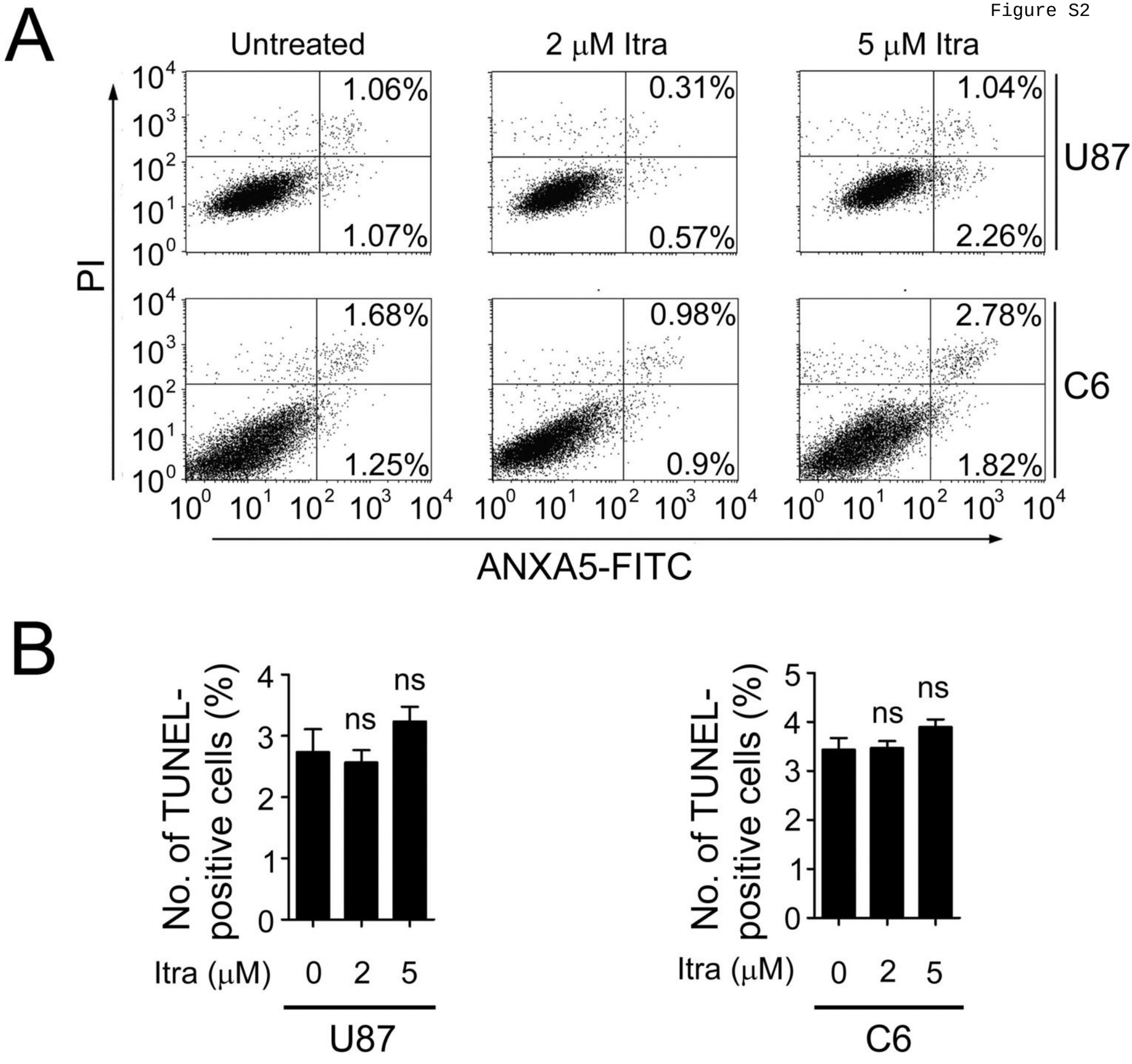
A
Untreated
2 μM Itra
5 μM Itra
1.06%
1.07%
0.31%
0.57%
1.04%
2.26%
U87
1.68%
1.25%
0.98%
0.9%
2.78%
1.82%
C6
PI
ANXA5-FITC
B
No. of TUNEL-positive cells (%)
ns
Itra (μM) 0 2 5
U87
C6

Figure S3

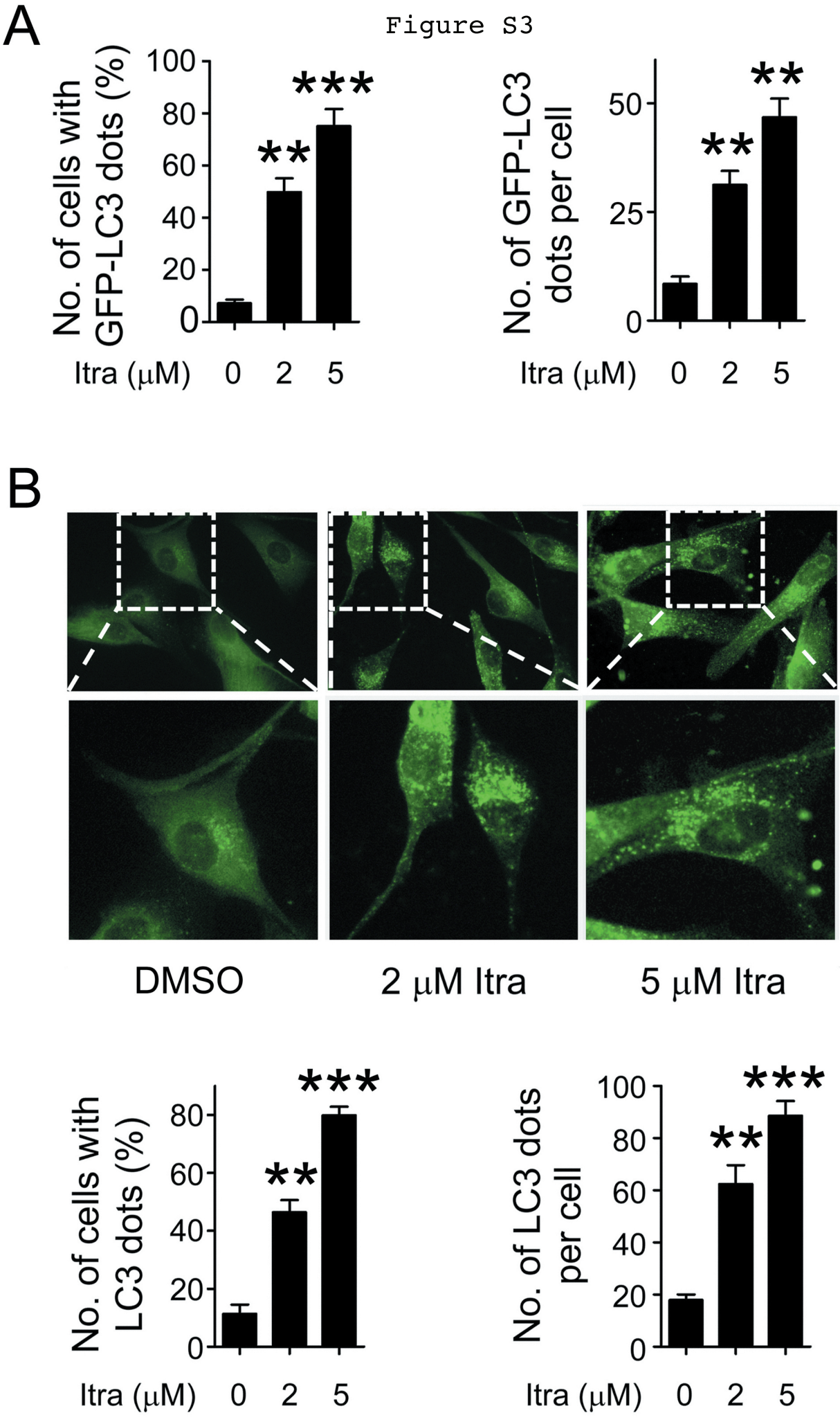
A
No. of cells with GFP-LC3 dots (%)
100
80
60
40
20
0
**
***
Itra (μM) 0 2 5
No. of GFP-LC3 dots per cell
50
25
0
**
**
Itra (μM) 0 2 5
B
DMSO
2 μM Itra
5 μM Itra
No. of cells with LC3 dots (%)
80
60
40
20
0
**
***
Itra (μM) 0 2 5
No. of LC3 dots per cell
100
80
60
40
20
0
**
***
Itra (μM) 0 2 5

Figure S4

A

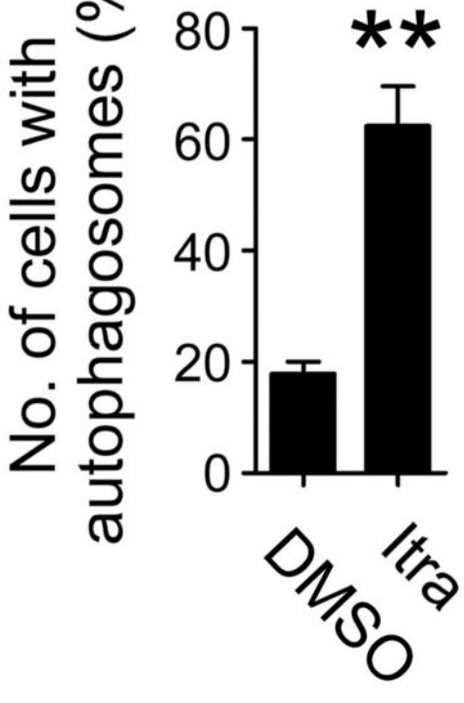
No. of cells with autophagosomes (%)
80
60
40
20
0
**
DMSO
Itra

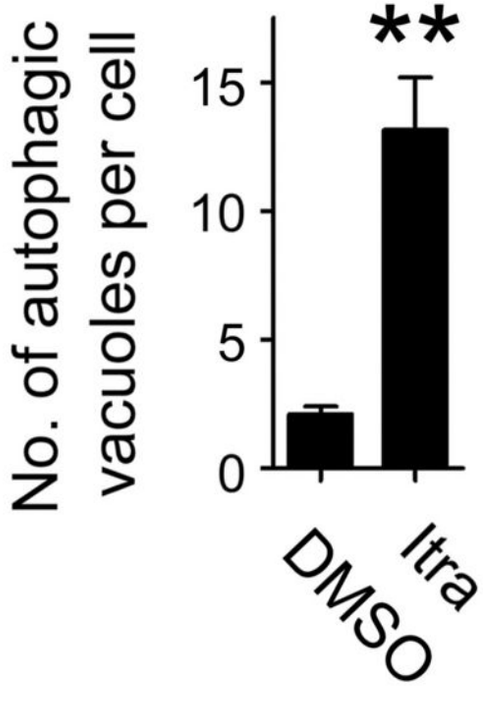
No. of autophagic vacuoles per cell
15
10
5
0
**
DMSO
Itra

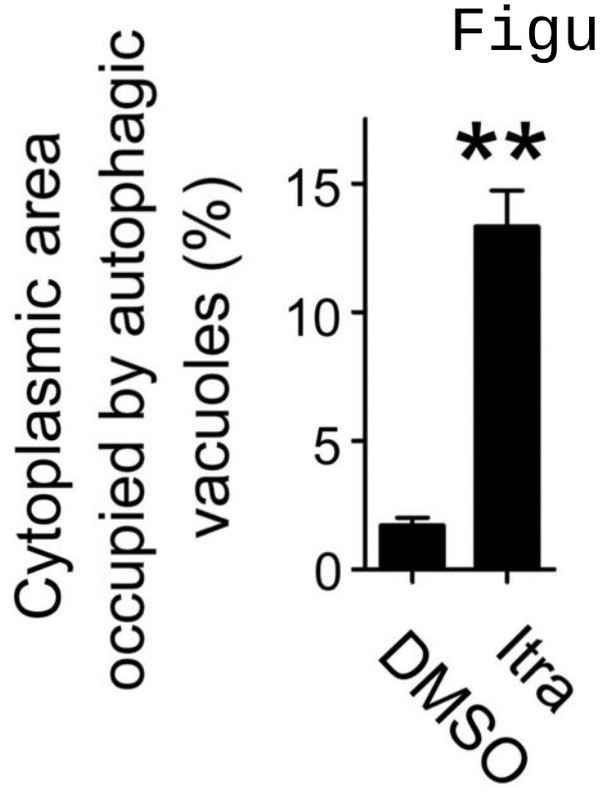
Cytoplasmic area occupied by autophagic vacuoles (%)
15
10
5
0
**
DMSO
Itra

B

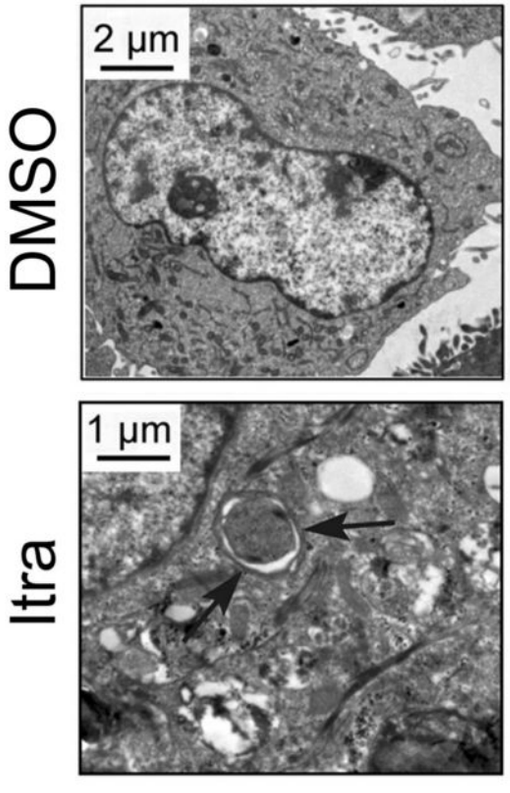
DMSO
2 µm
Itra
1 µm

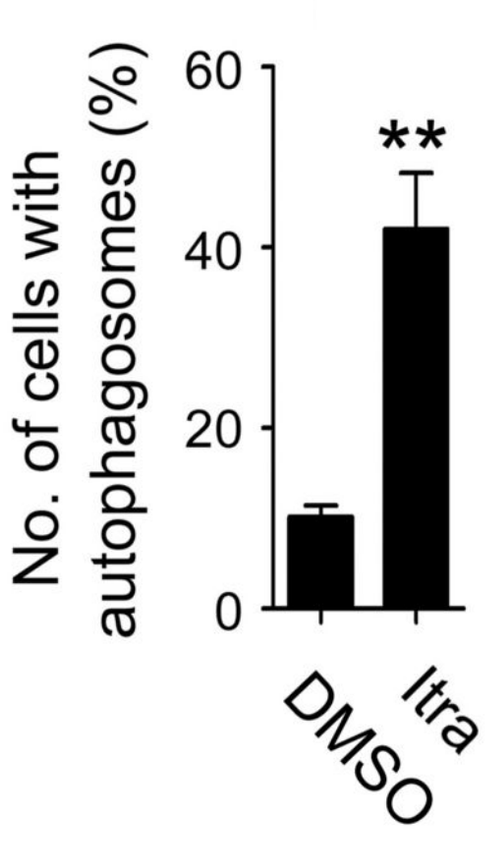
No. of cells with autophagosomes (%)
60
40
20
0
**
DMSO
Itra

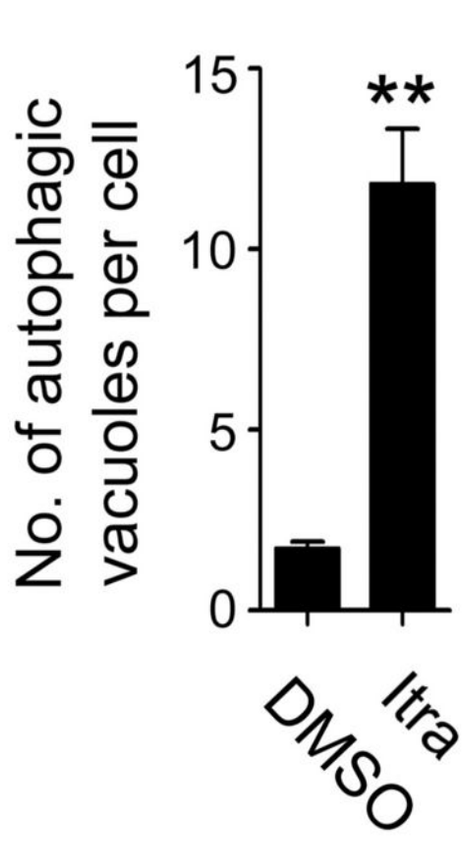
No. of autophagic vacuoles per cell
15
10
5
0
**
DMSO
Itra

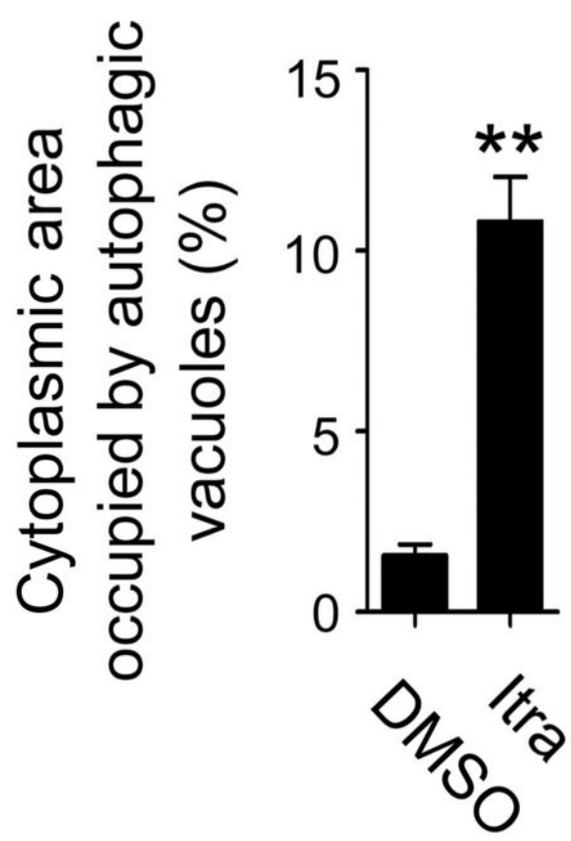
Cytoplasmic area occupied by autophagic vacuoles (%)
15
10
5
0
**
DMSO
Itra

Figure S5

A

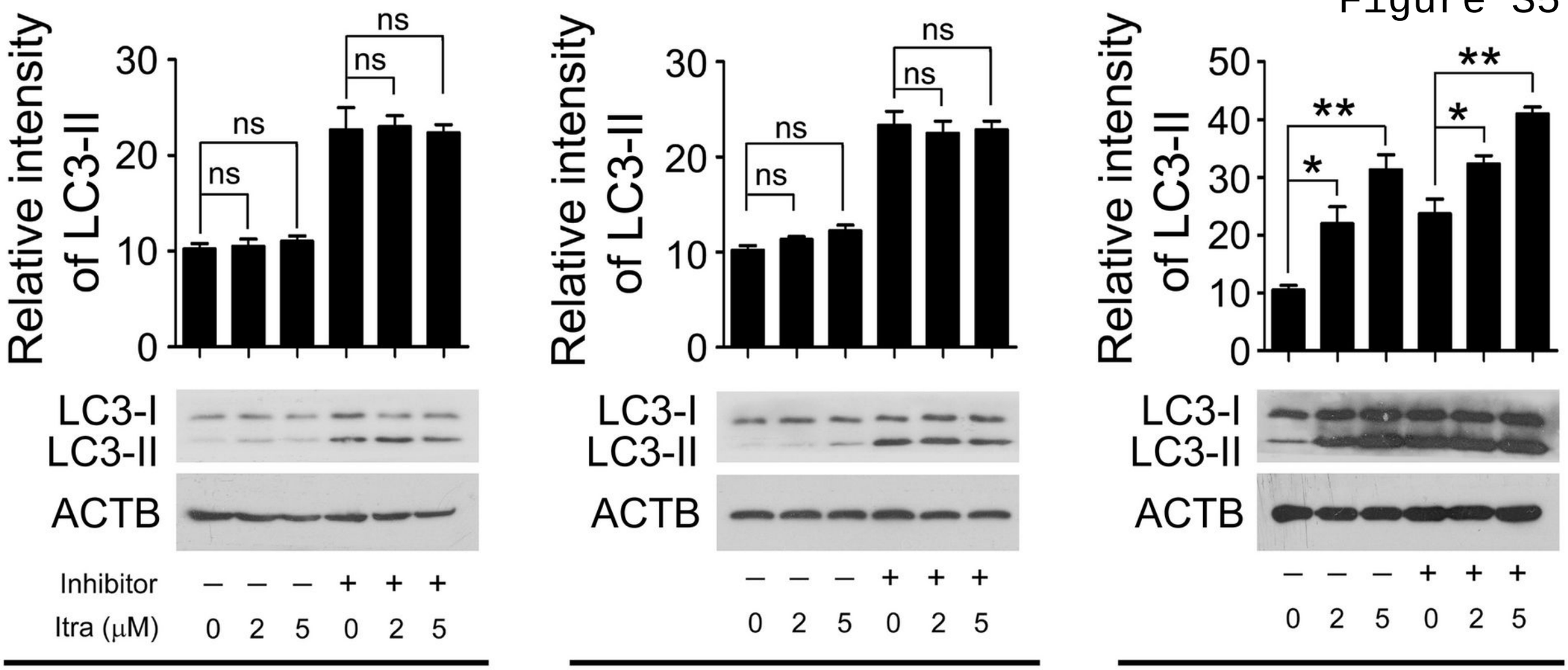

B

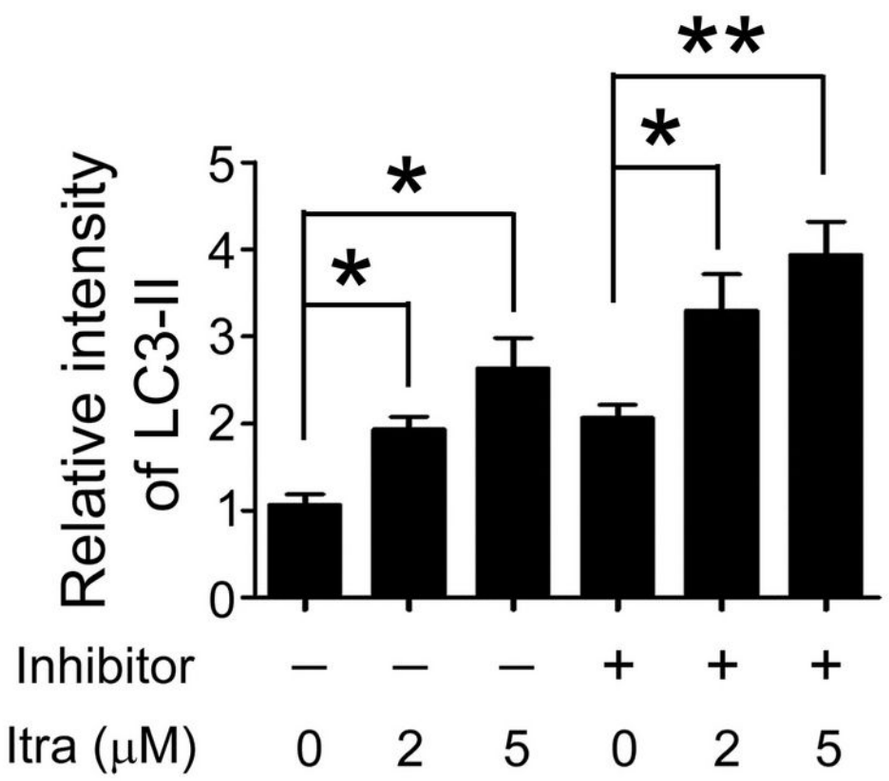

D

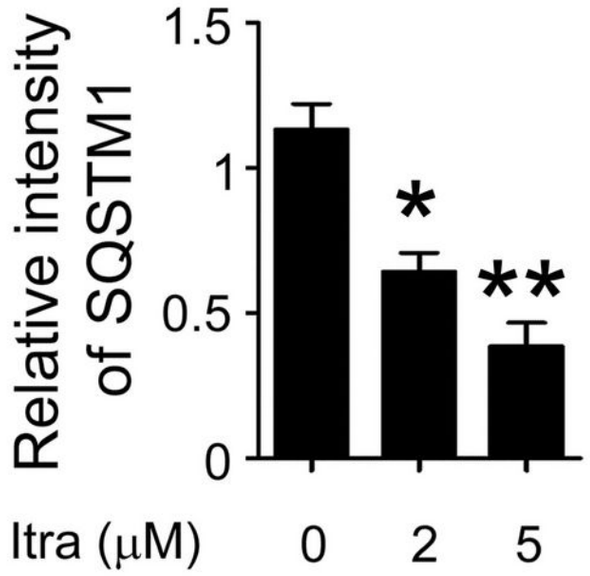

C

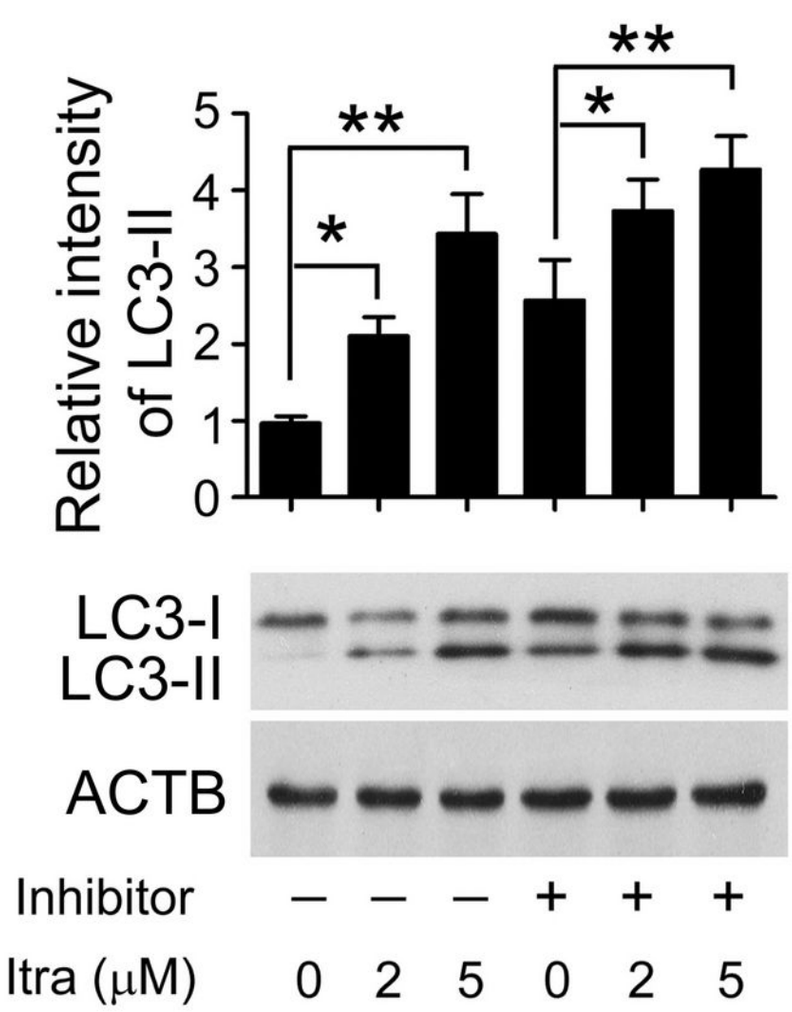

E

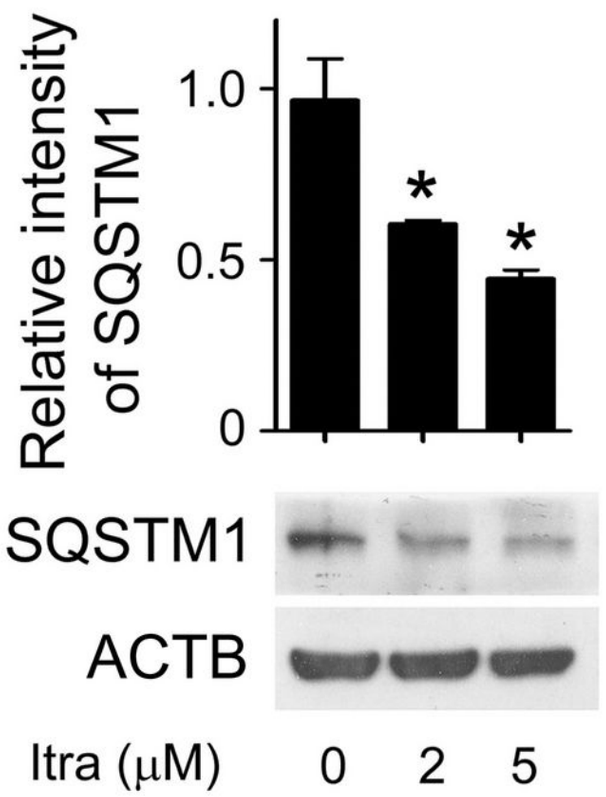

Figure S6

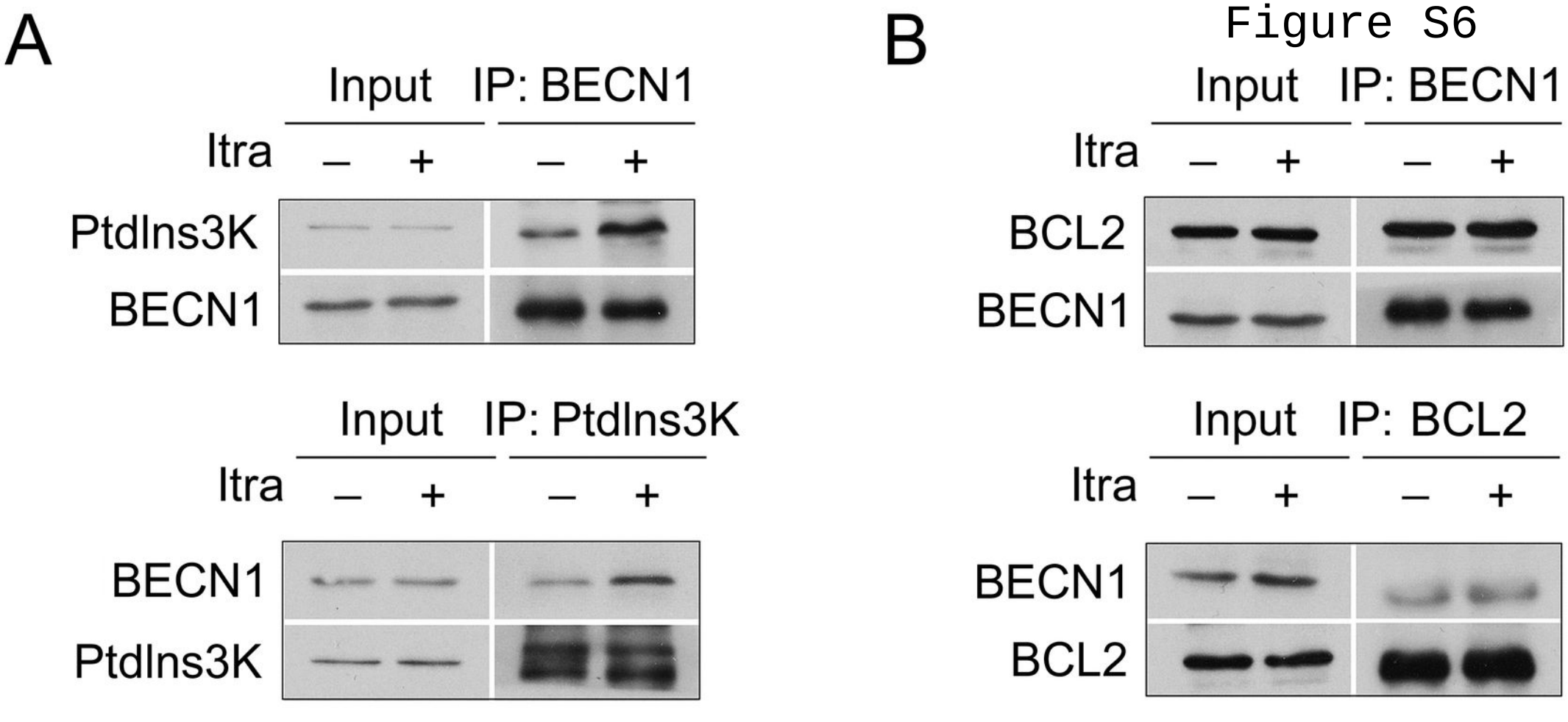
A
Input
IP: BECN1
Itra
–
+
–
+
PtdIns3K
BECN1
Input
IP: PtdIns3K
Itra
–
+
–
+
BECN1
PtdIns3K
B
Input
IP: BECN1
Itra
–
+
–
+
BCL2
BECN1
Input
IP: BCL2
Itra
–
+
–
+
BECN1
BCL2
C
Input
IP: BECN1
Itra
–
+
–
+
ATG14
BECN1
Input
IP: ATG14
Itra
–
+
–
+
BECN1
ATG14
D
Relative intensity of LC3-II
2.5
2.0
1.5
1.0
0.5
0
*
Vehicle
Itra

Figure S7

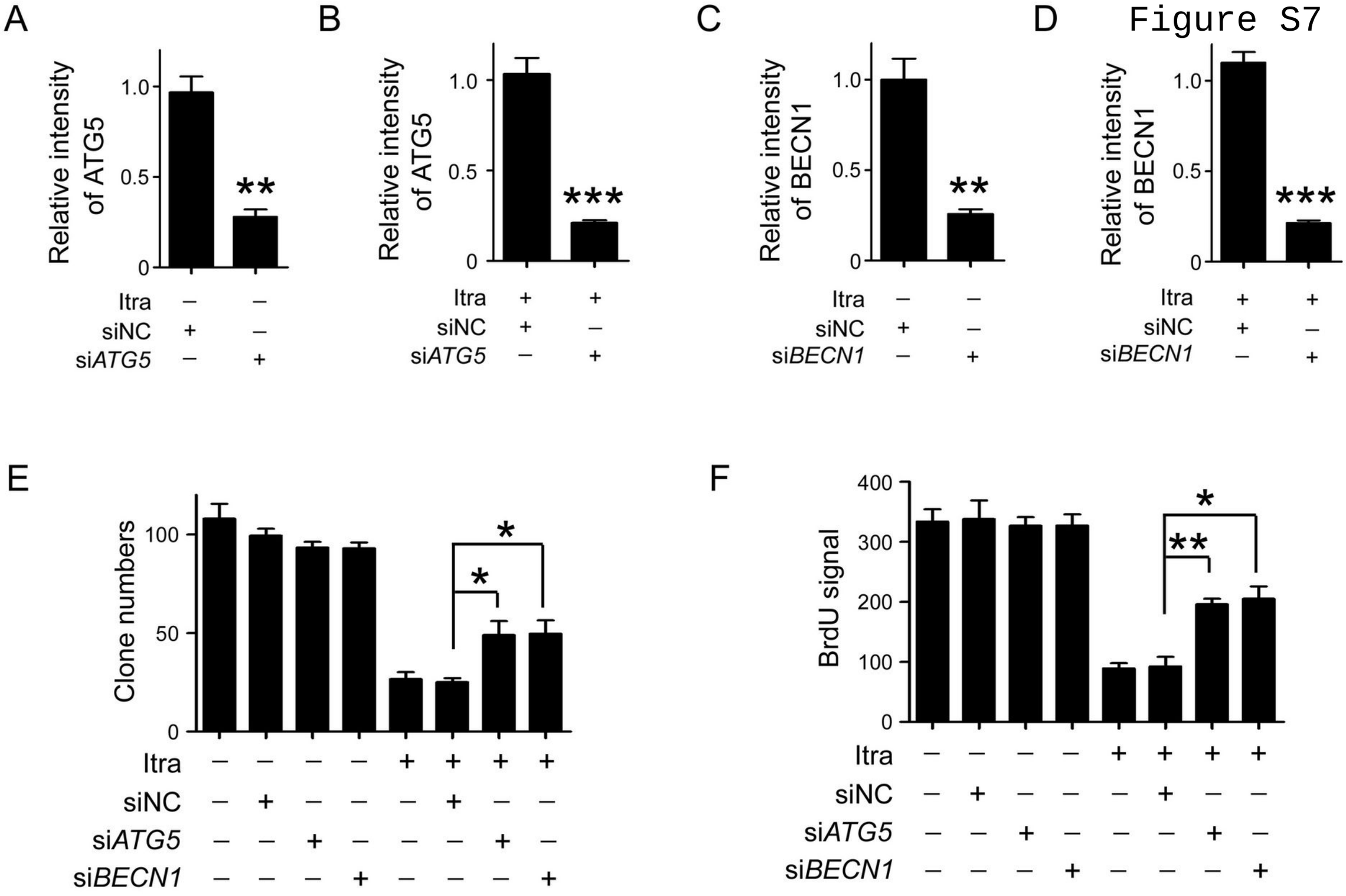
A
Relative intensity of ATG5
1.0
0.5
0
**
Itra – –
siNC + –
siATG5 – +
B
Relative intensity of ATG5
1.0
0.5
0
***
Itra + +
siNC + –
siATG5 – +
C
Relative intensity of BECN1
1.0
0.5
0
**
Itra – –
siNC + –
siBECN1 – +
D
Relative intensity of BECN1
1.0
0.5
0
***
Itra + +
siNC + –
siBECN1 – +
E
Clone numbers
100
50
0
*
*
Itra – – – – + + + +
siNC – + – – – + – –
siATG5 – – + – – – + –
siBECN1 – – – + – – – +
F
BrdU signal
400
300
200
100
0
*
**
Itra – – – – + + + +
siNC – + – – – + – –
siATG5 – – + – – – + –
siBECN1 – – – + – – – +

Figure S8

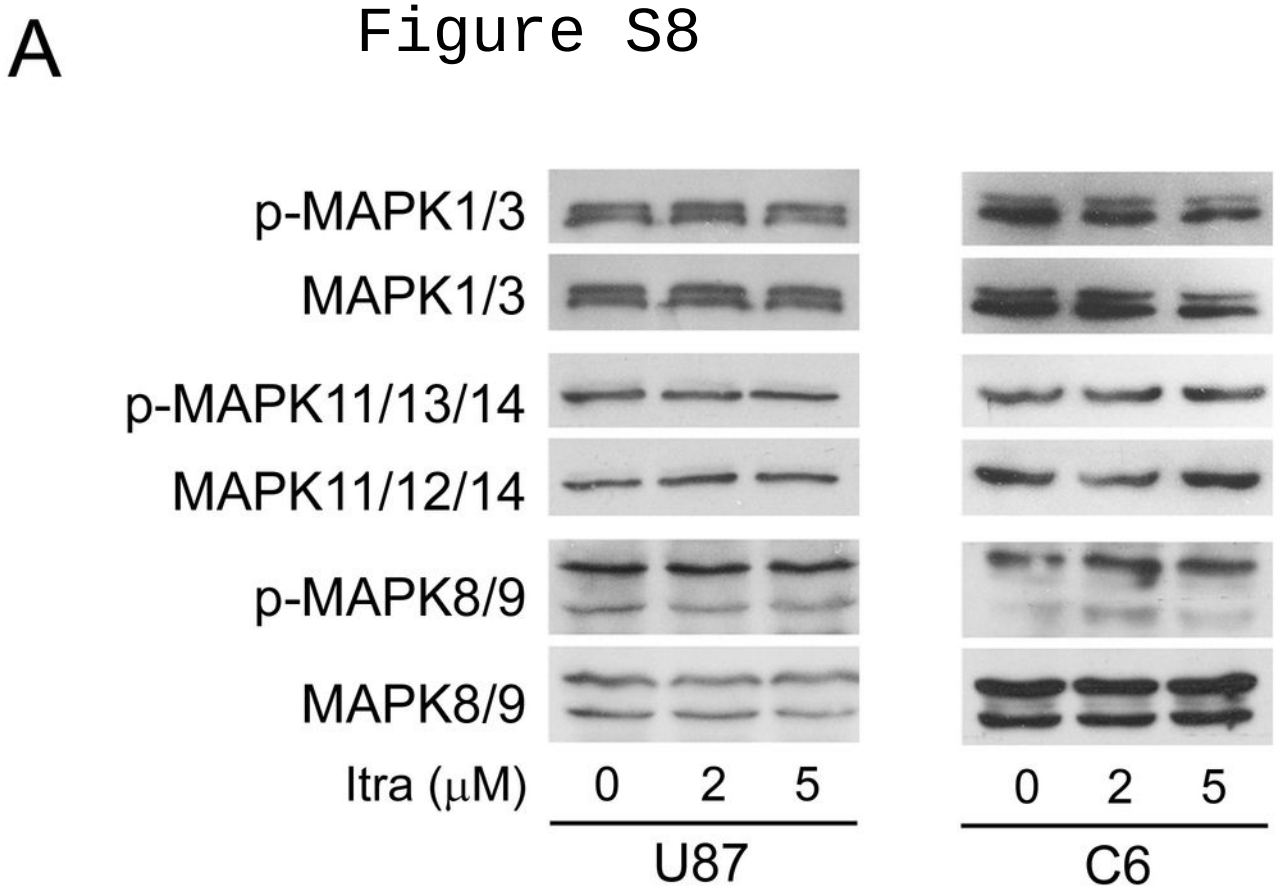
A
p-MAPK1/3
MAPK1/3
p-MAPK11/13/14
MAPK11/12/14
p-MAPK8/9
MAPK8/9
Itra (μM)
0 2 5
0 2 5
U87
C6
B
HA
ACTB
p-MTOR
MTOR
p-CDKN1A
CDKN1A
p-CDKN1B
CDKN1B
Itra – + +
Mock – + –
ca-AKT1 – – +
C
No. of cells with LC3 dots (%)
100
80
60
40
20
0
**
Itra – + +
Mock – + –
ca-AKT1 – – +
No. of LC3 dots per cells
80
60
40
20
0
*
Itra – + +
Mock – + –
ca-AKT1 – – +
D
Percentage of cells with S phase
30
20
10
0
*
Itra – + + + + + + +
Mock – – + – – – + –
ca-AKT1 – – – + – – – +
siNC – – – – + – – –
siBECN1 – – – – – + + +

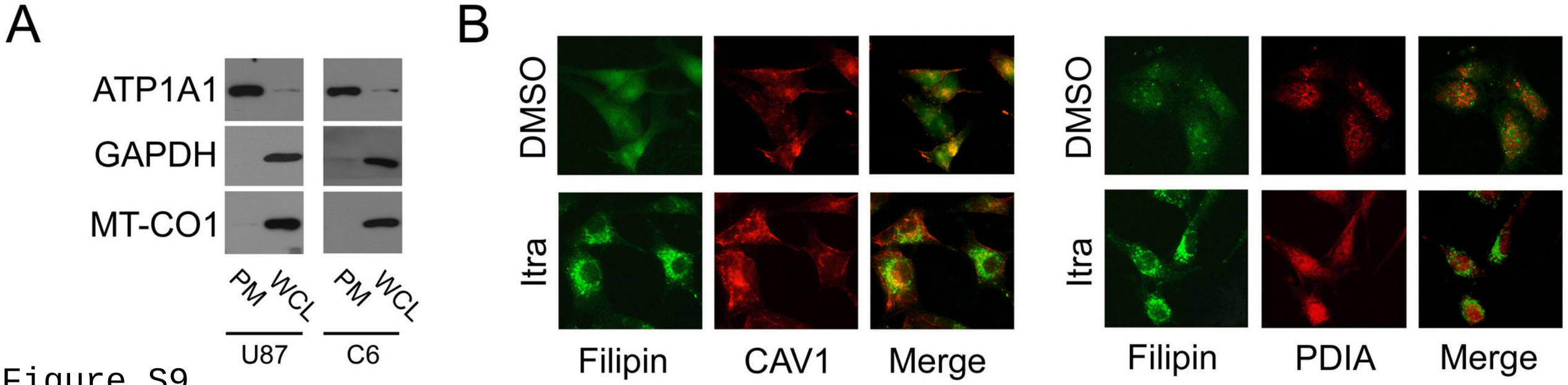
A
ATP1A1
GAPDH
MT-CO1
PM
WCL
PM
WCL
U87
C6
B
DMSO
Itra
Filipin
CAV1
Merge
DMSO
Itra
Filipin
PDIA
Merge

Figure S9

Figure S10

A

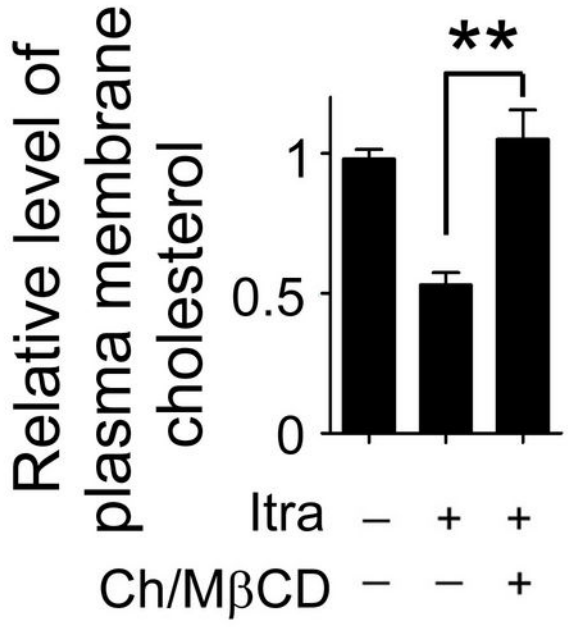

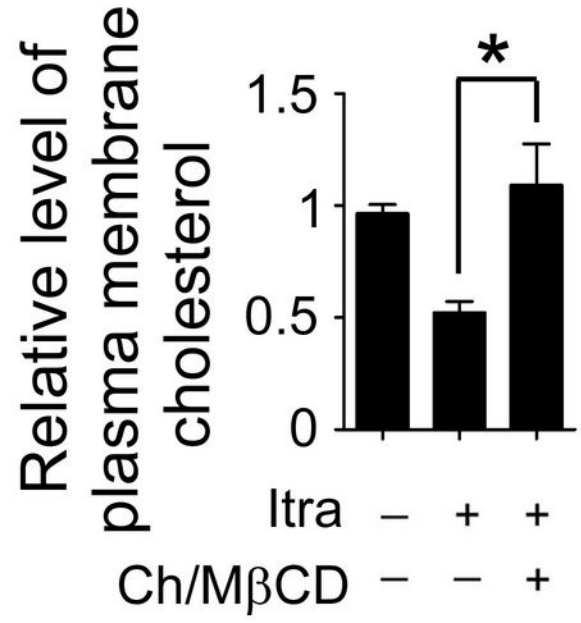

B

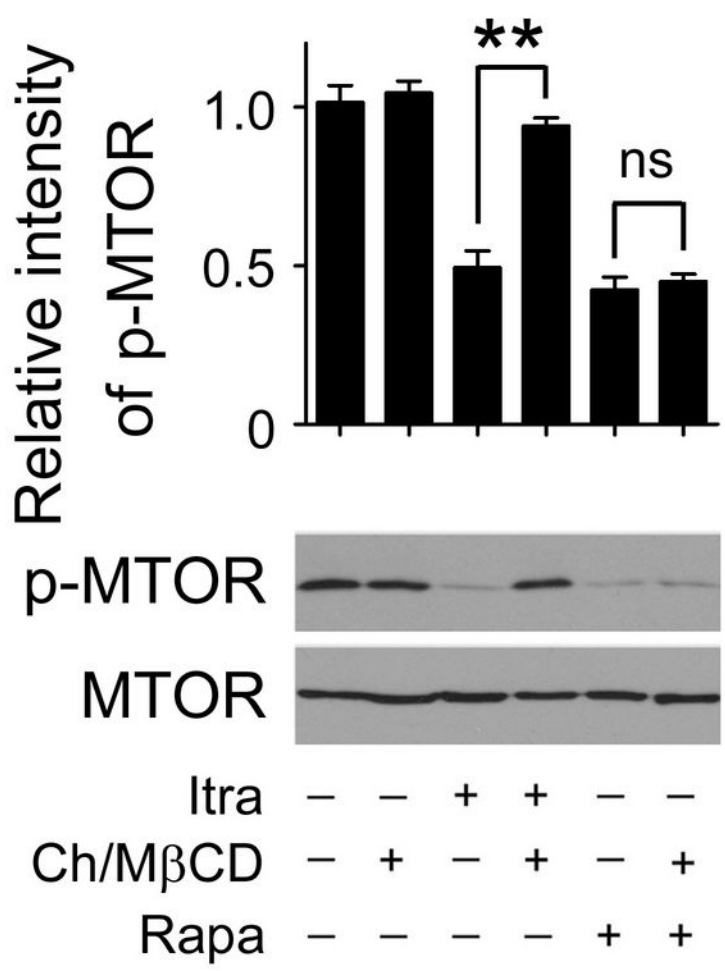

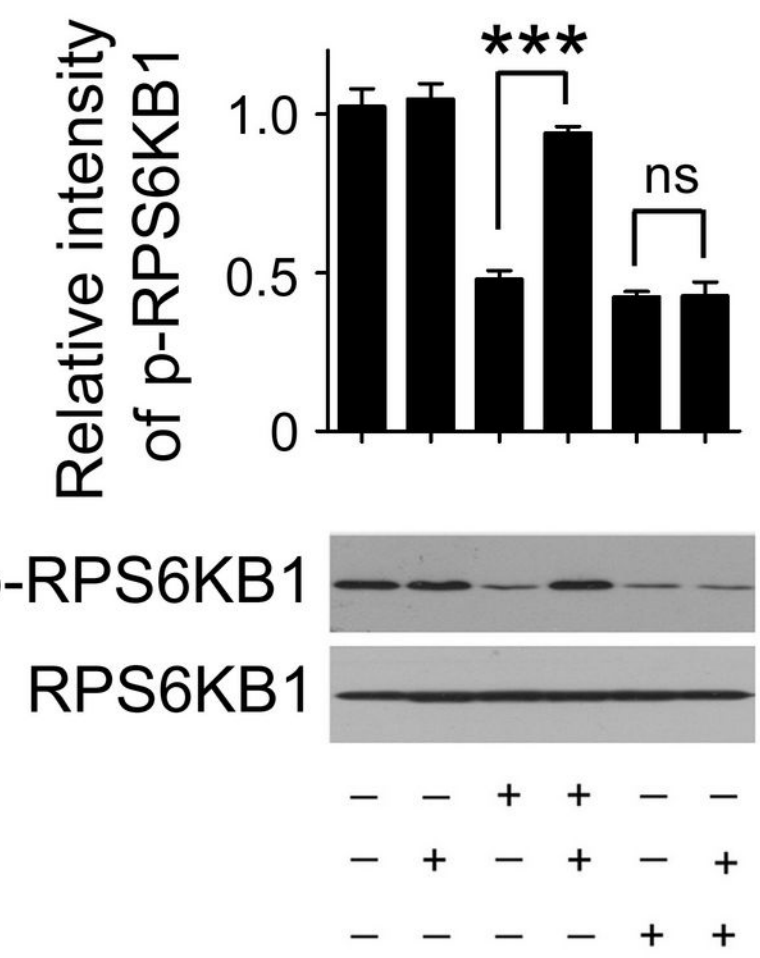

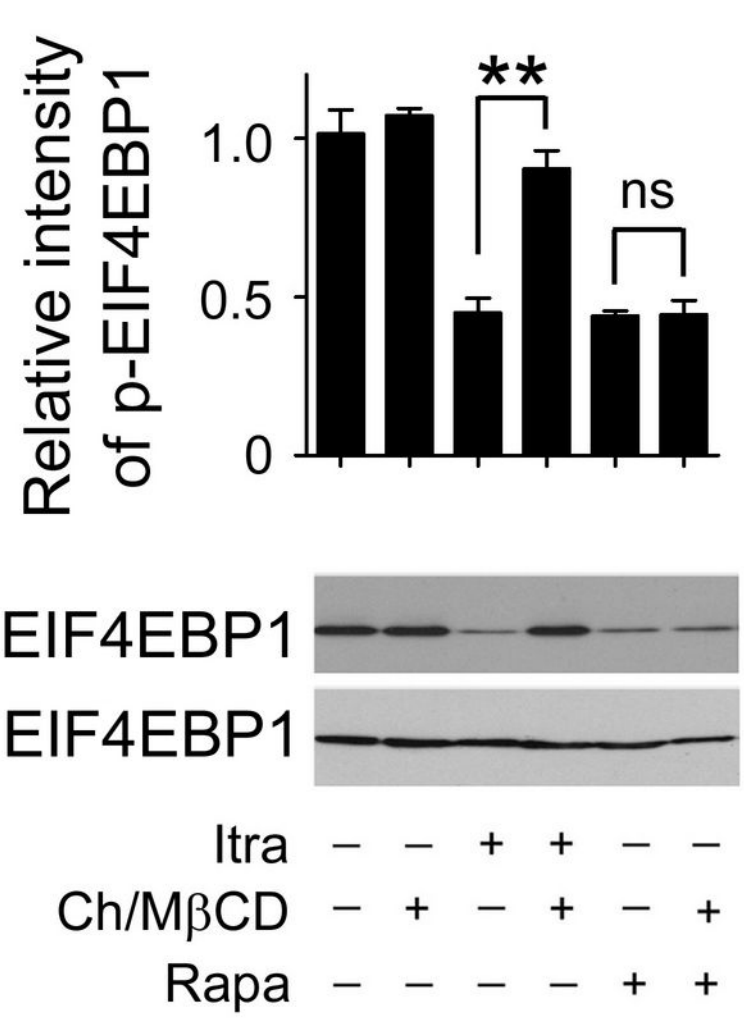

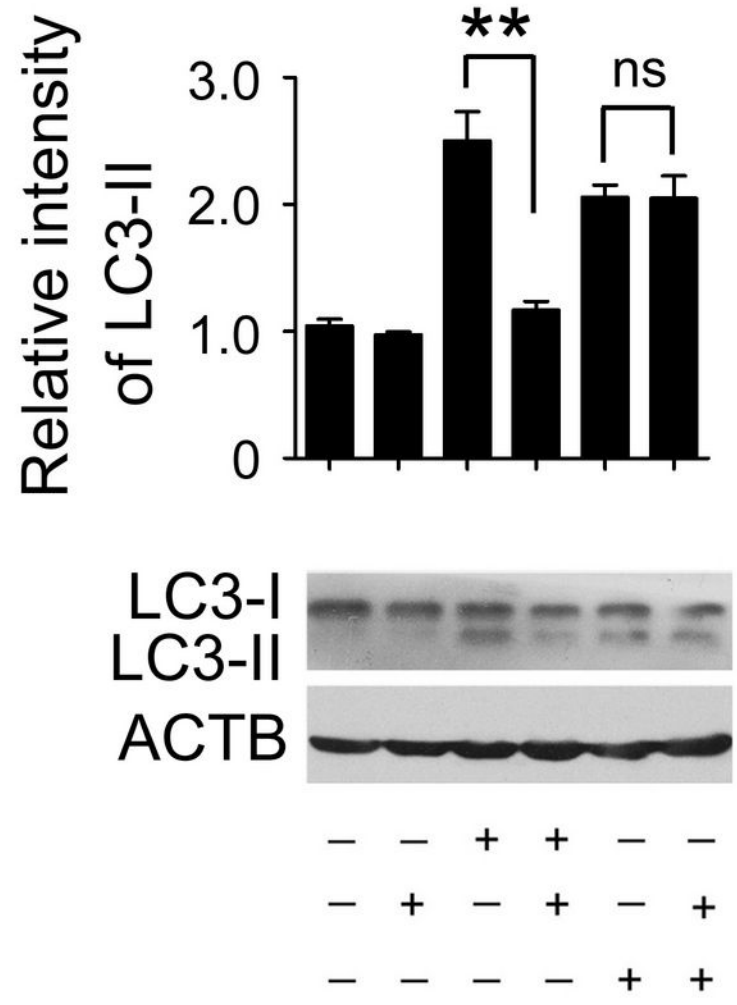

Figure S11

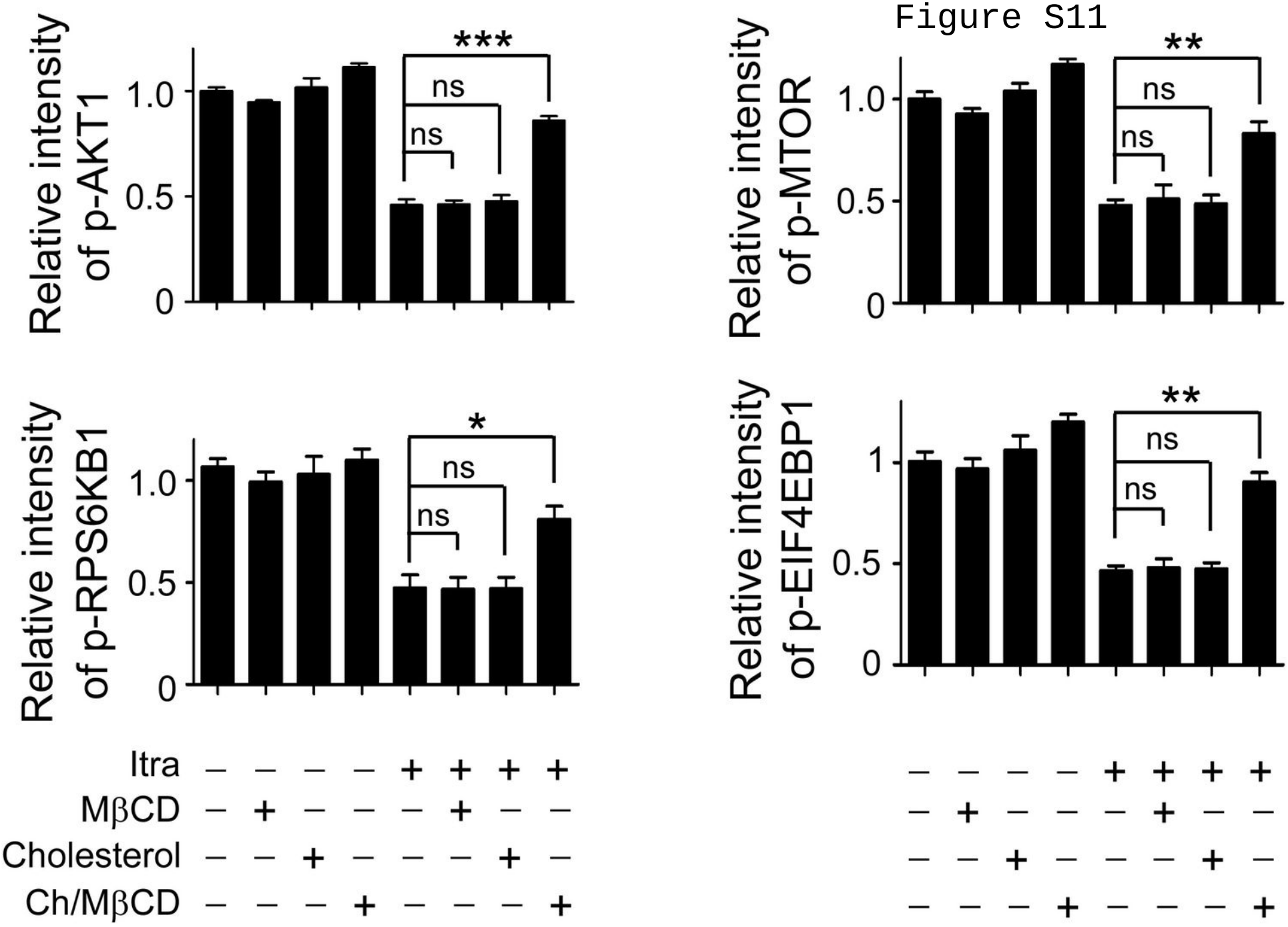
Relative intensity of p-AKT1
***
ns
ns
1.0
0.5
0
Relative intensity of p-MTOR
**
ns
ns
1.0
0.5
0
Relative intensity of p-RPS6KB1
*
ns
ns
1.0
0.5
0
Relative intensity of p-EIF4EBP1
**
ns
ns
1
0.5
0
Itra – – – – + + + +
MβCD – + – – – + – –
Cholesterol – – + – – – + –
Ch/MβCD – – – + – – – +
– – – – + + + +
– + – – – + – –
– – + – – – + –
– – – + – – – +

Figure S12

A

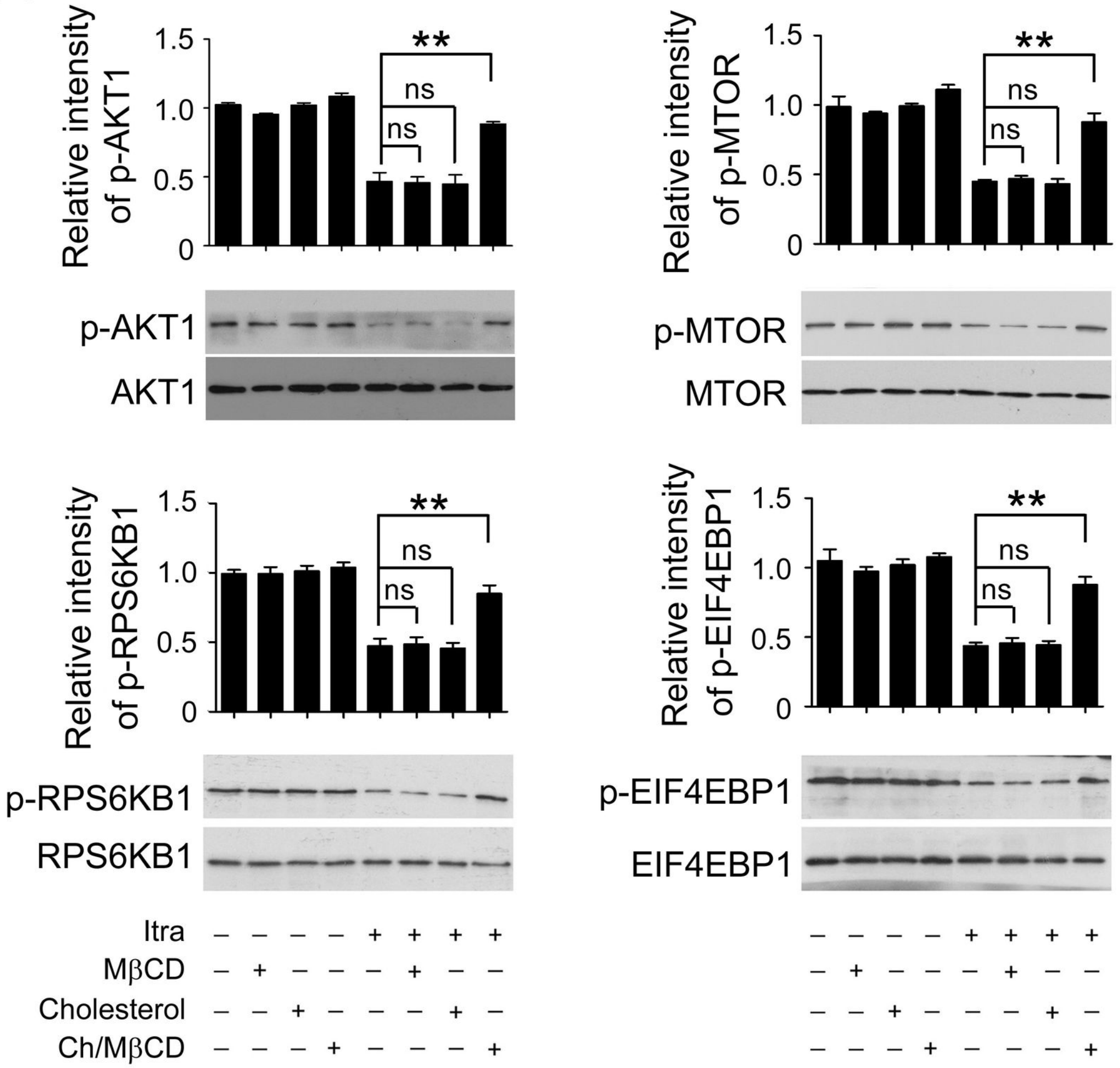

B

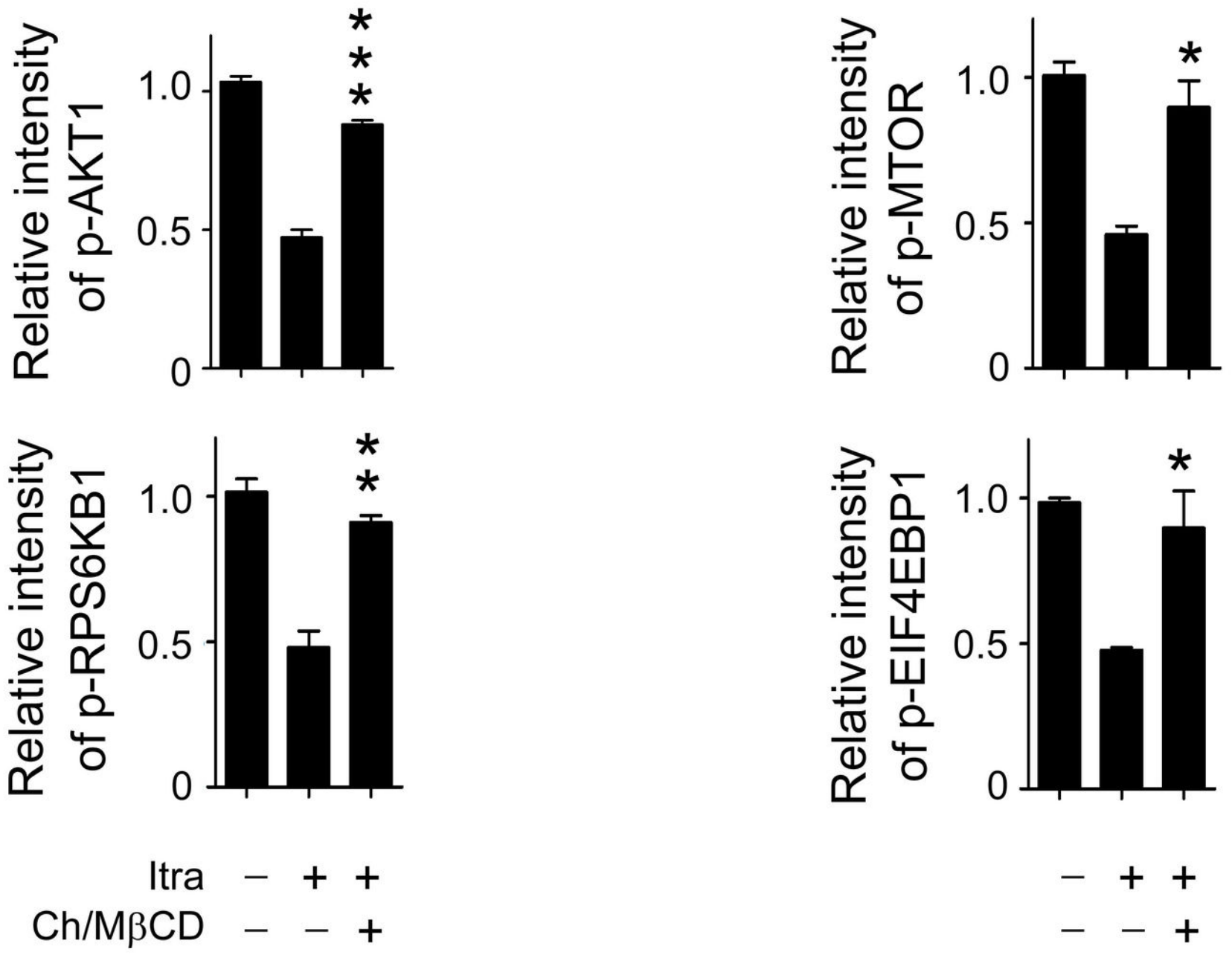

Figure S13

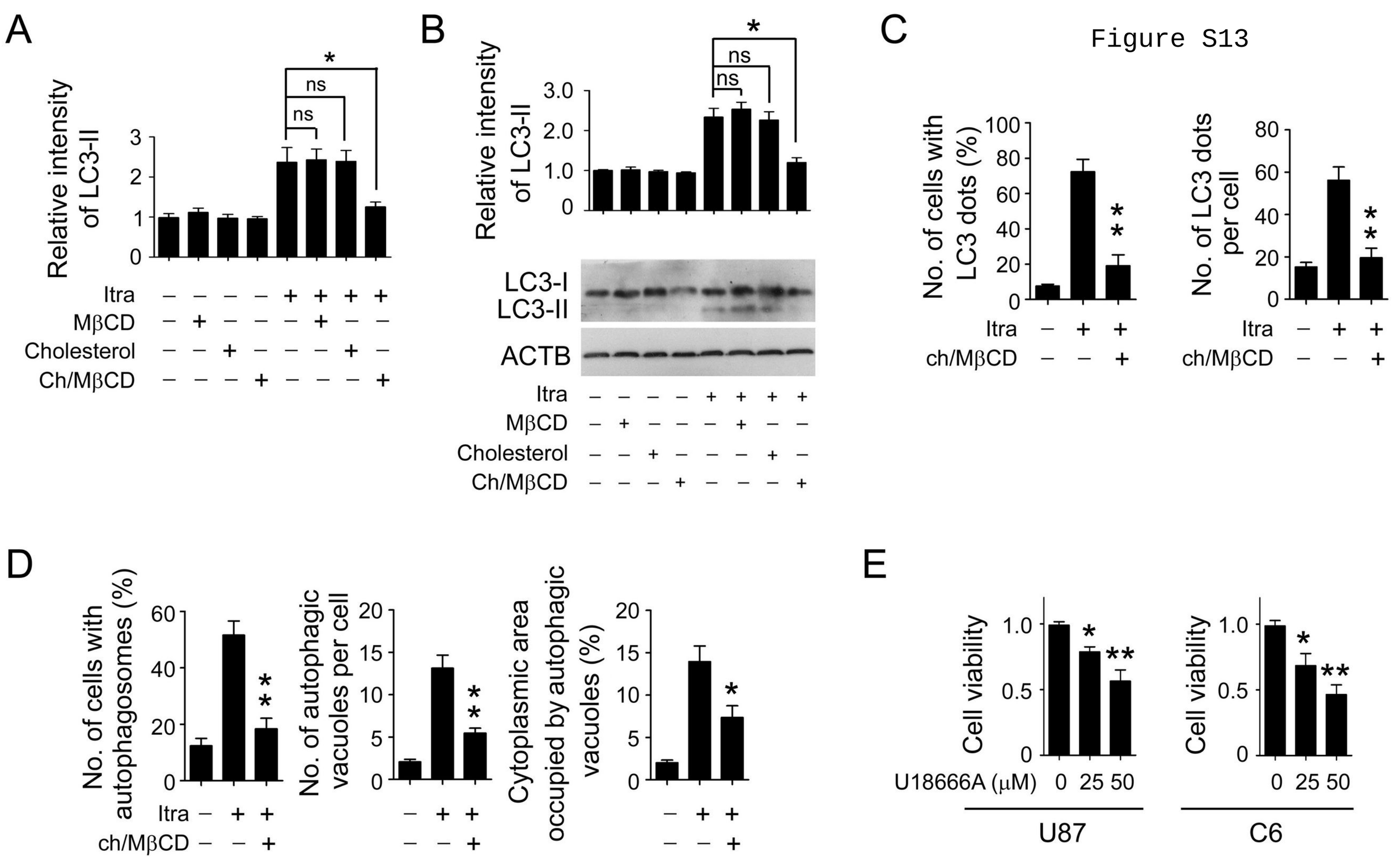
A
Relative intensity of LC3-II
3
2
1
0
*
ns
ns
Itra – – – – + + + +
MβCD – + – – – + – –
Cholesterol – – + – – – + –
Ch/MβCD – – – + – – – +
B
Relative intensity of LC3-II
3.0
2.0
1.0
0
*
ns
ns
LC3-I
LC3-II
ACTB
Itra – – – – + + + +
MβCD – + – – – + – –
Cholesterol – – + – – – + –
Ch/MβCD – – – + – – – +
C
No. of cells with LC3 dots (%)
100
80
60
40
20
0
**
Itra – + +
ch/MβCD – – +
No. of LC3 dots per cell
80
60
40
20
0
**
Itra – + +
ch/MβCD – – +
D
No. of cells with autophagosomes (%)
60
40
20
0
**
Itra – + +
ch/MβCD – – +
No. of autophagic vacuoles per cell
20
15
10
5
0
**
– + +
– – +
Cytoplasmic area occupied by autophagic vacuoles (%)
20
15
10
5
0
*
– + +
– – +
E
Cell viability
1.0
0.5
0
*
**
U18666A (μM) 0 25 50
U87
Cell viability
1.0
0.5
0
*
**
0 25 50
C6

Figure S14

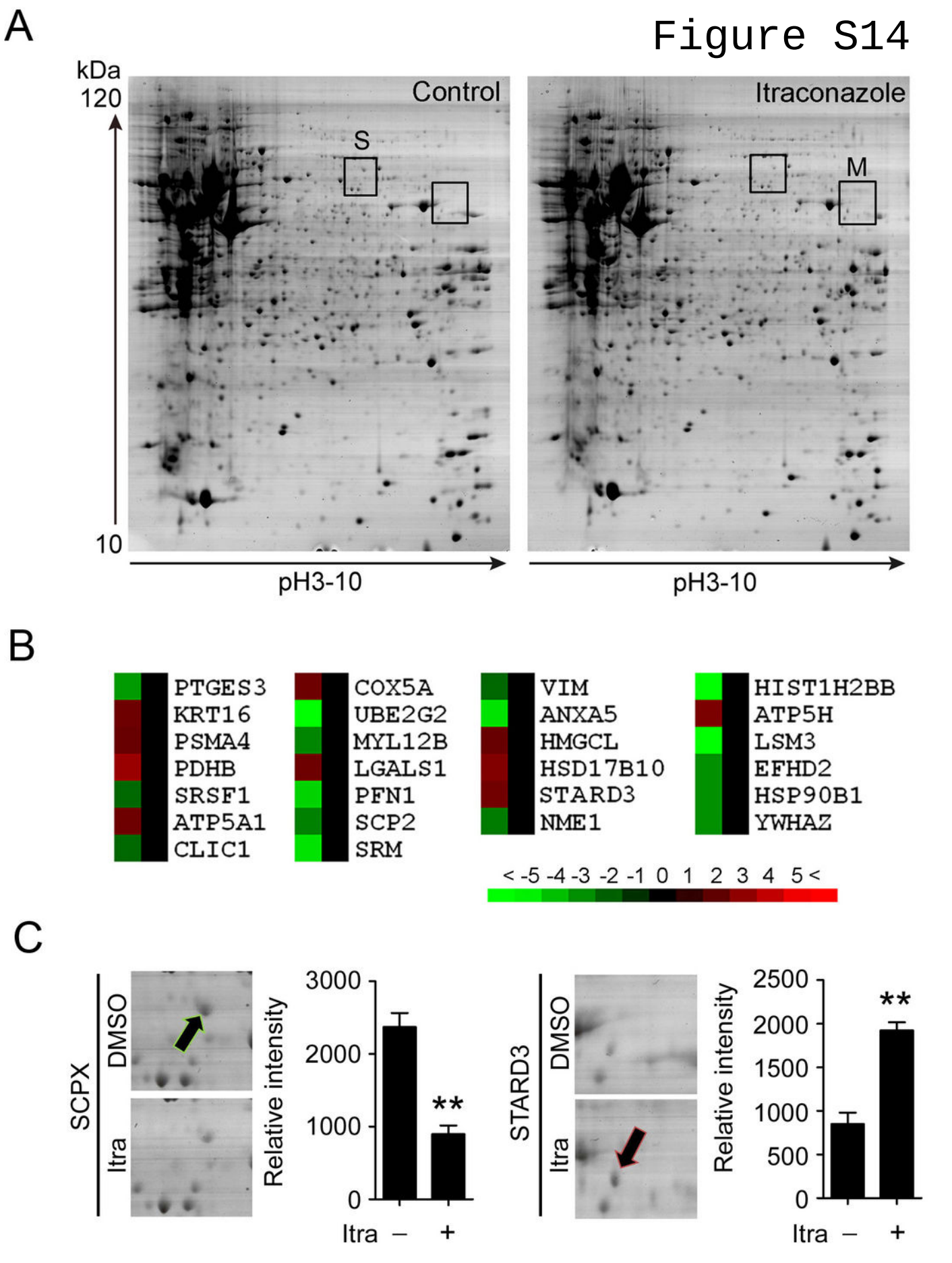
A
kDa
120
10
Control
Itraconazole
S
M
pH3-10
pH3-10
B
PTGES3
KRT16
PSMA4
PDHB
SRSF1
ATP5A1
CLIC1
COX5A
UBE2G2
MYL12B
LGALS1
PFN1
SCP2
SRM
VIM
ANXA5
HMGCL
HSD17B10
STARD3
NME1
HIST1H2BB
ATP5H
LSM3
EFHD2
HSP90B1
YWHAZ
< -5 -4 -3 -2 -1 0 1 2 3 4 5 <
C
SCPX
DMSO
Itra
Relative intensity
3000
2000
1000
0
**
Itra – +
STARD3
DMSO
Itra
Relative intensity
2500
2000
1500
1000
500
0
**
Itra – +

Figure S15

A

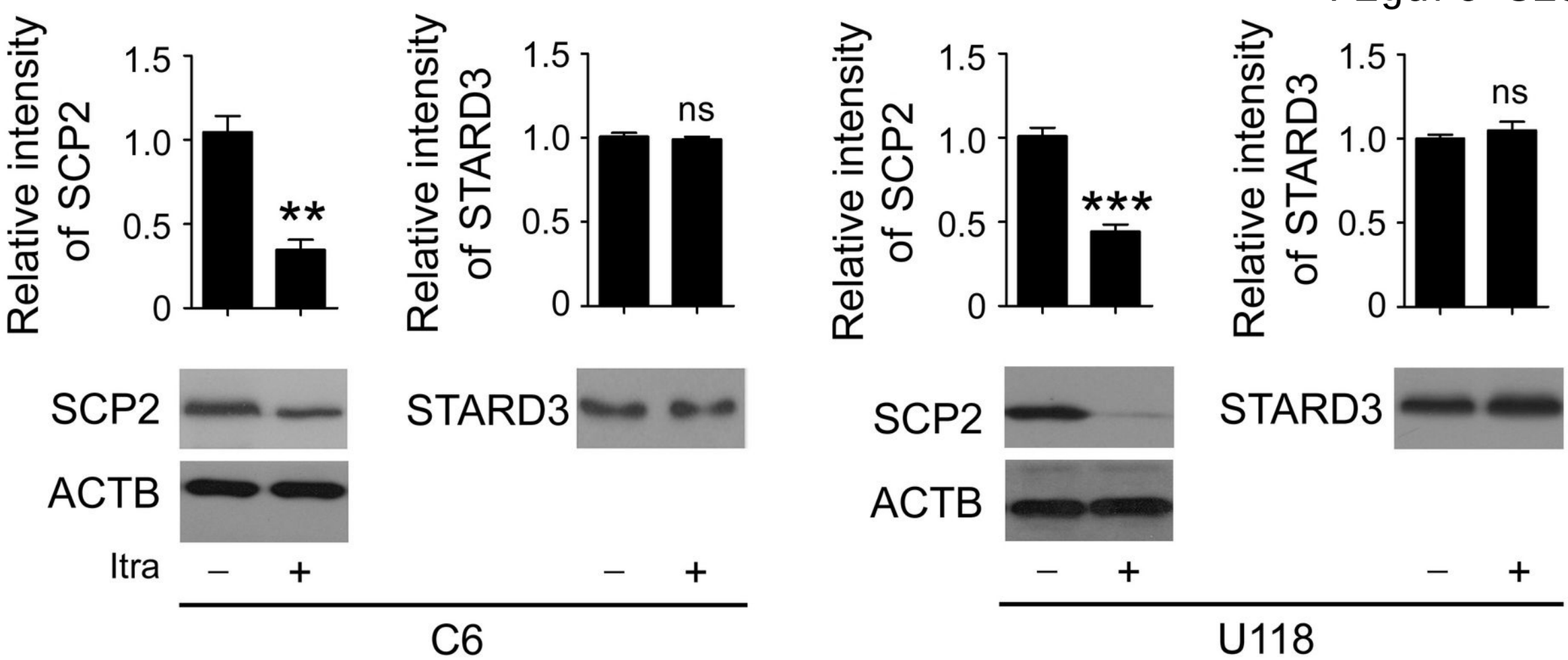

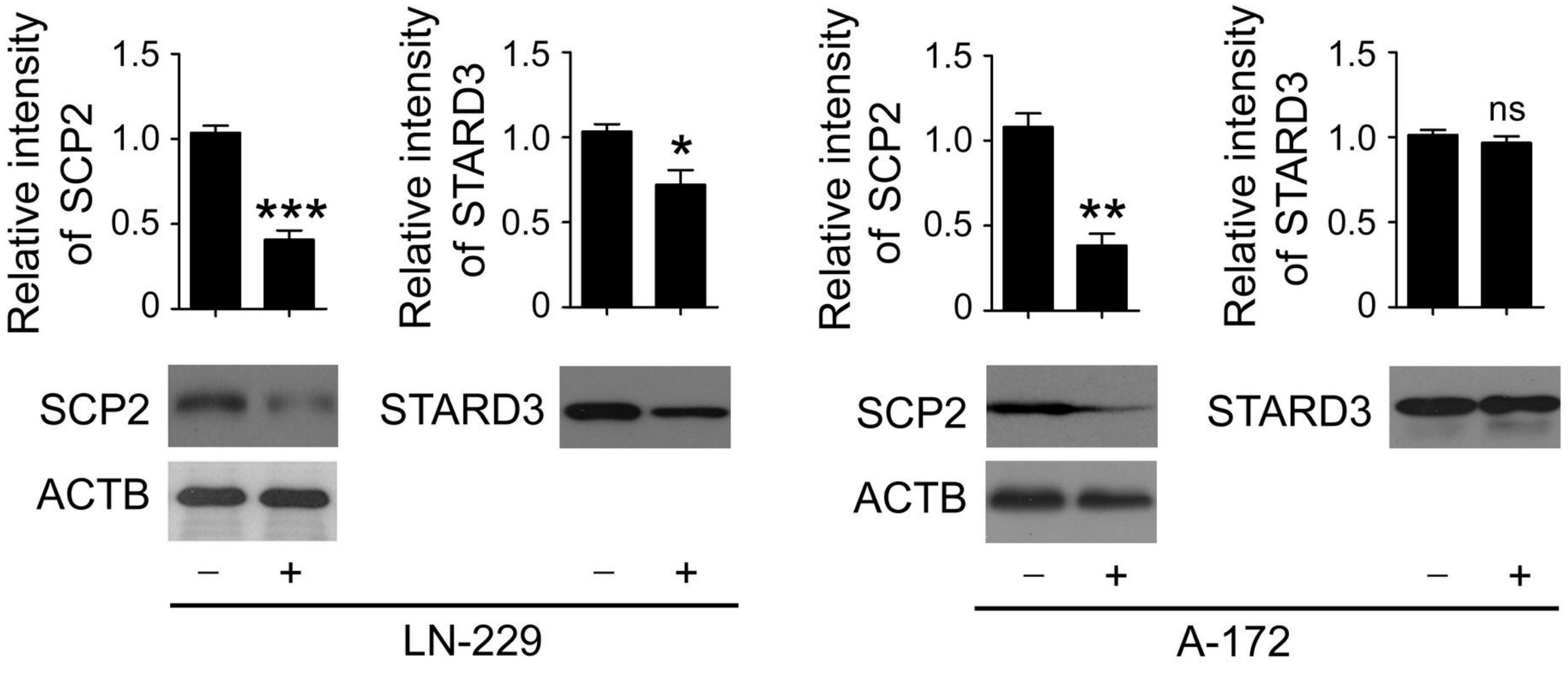

B

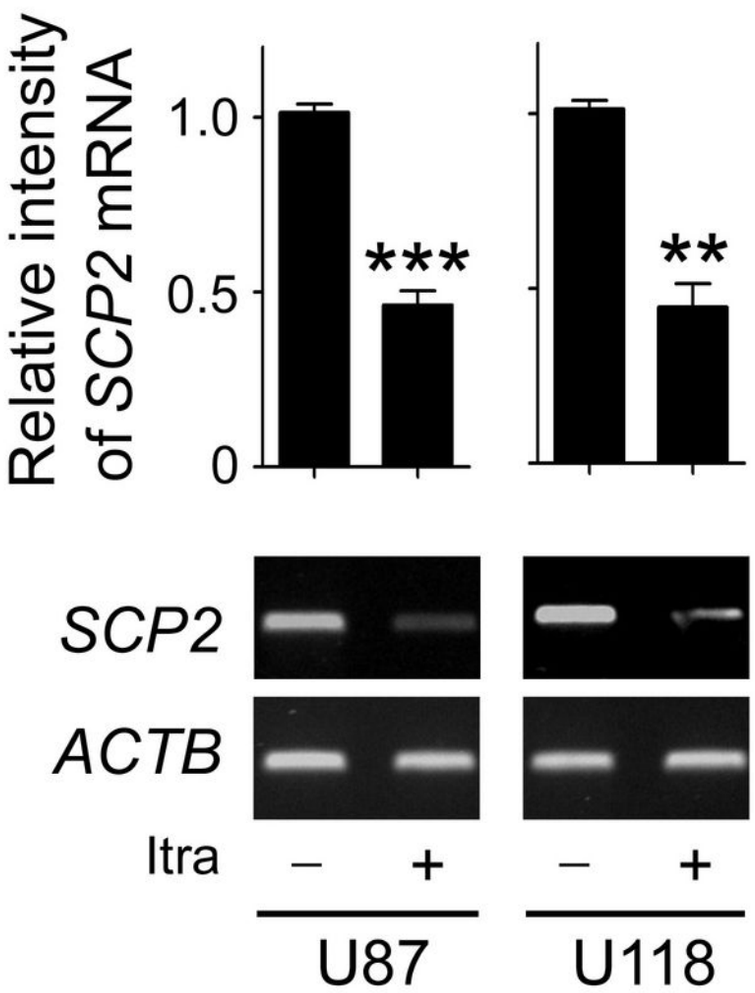

C

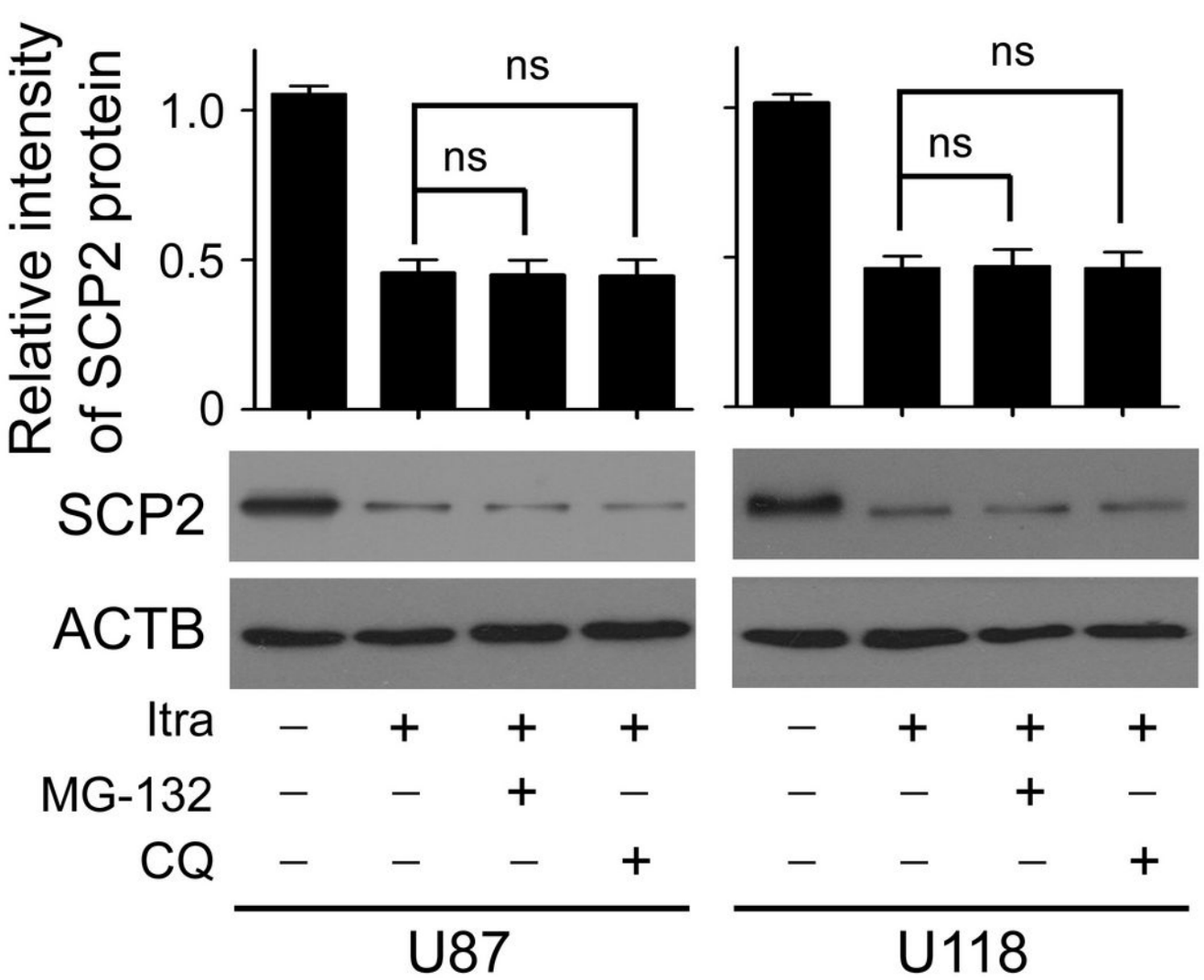

Figure S16

A

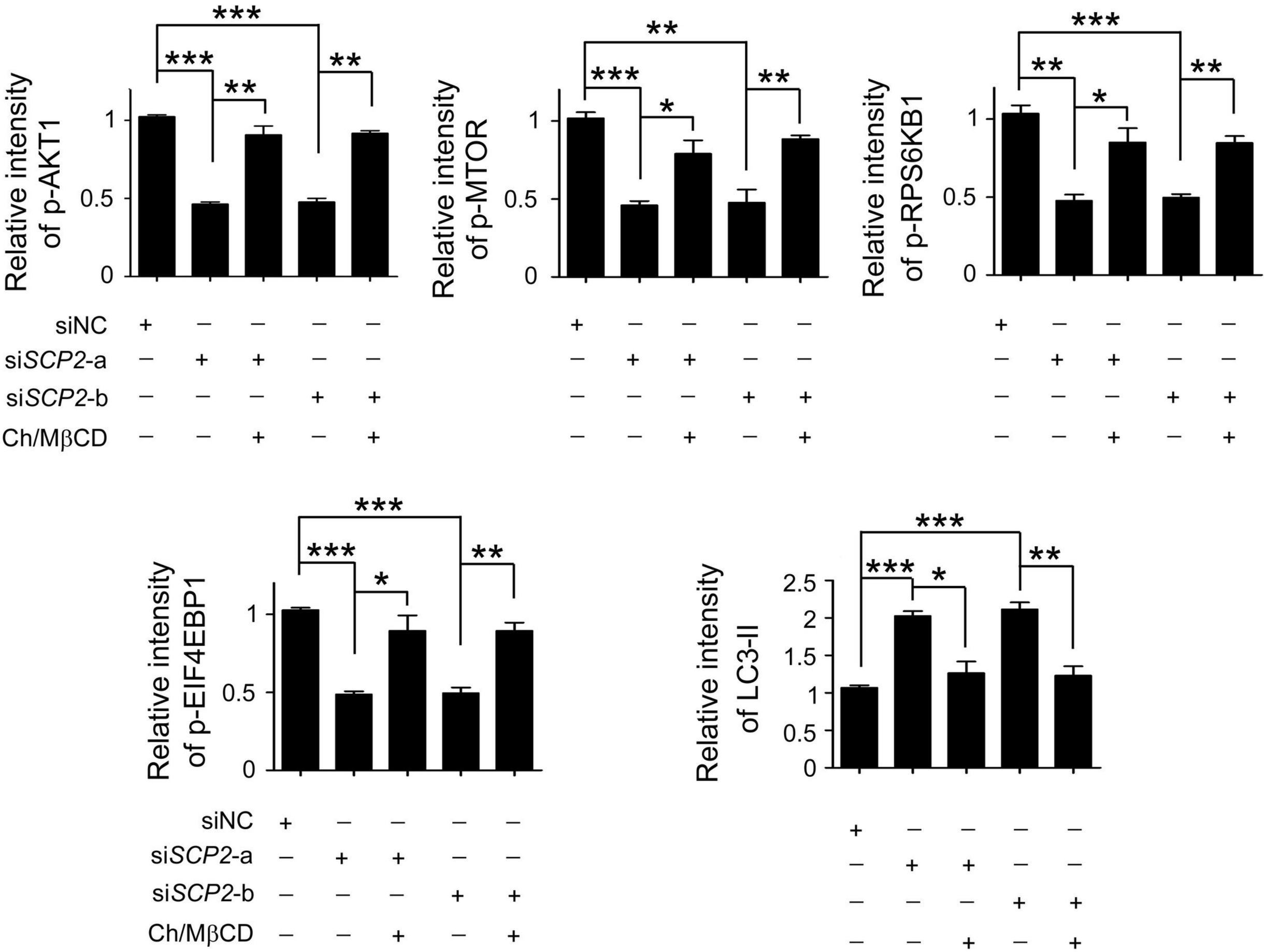

B

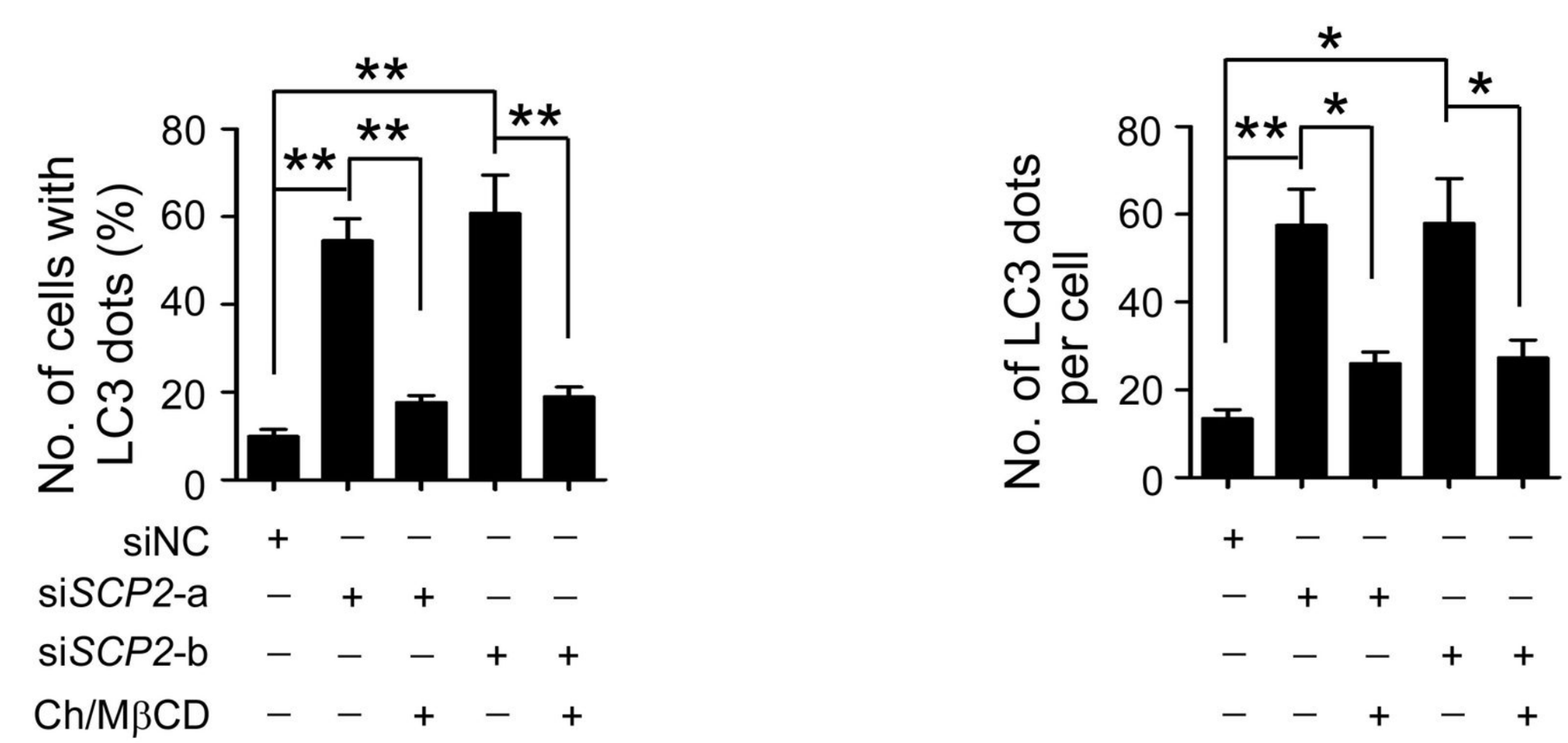

Figure S17

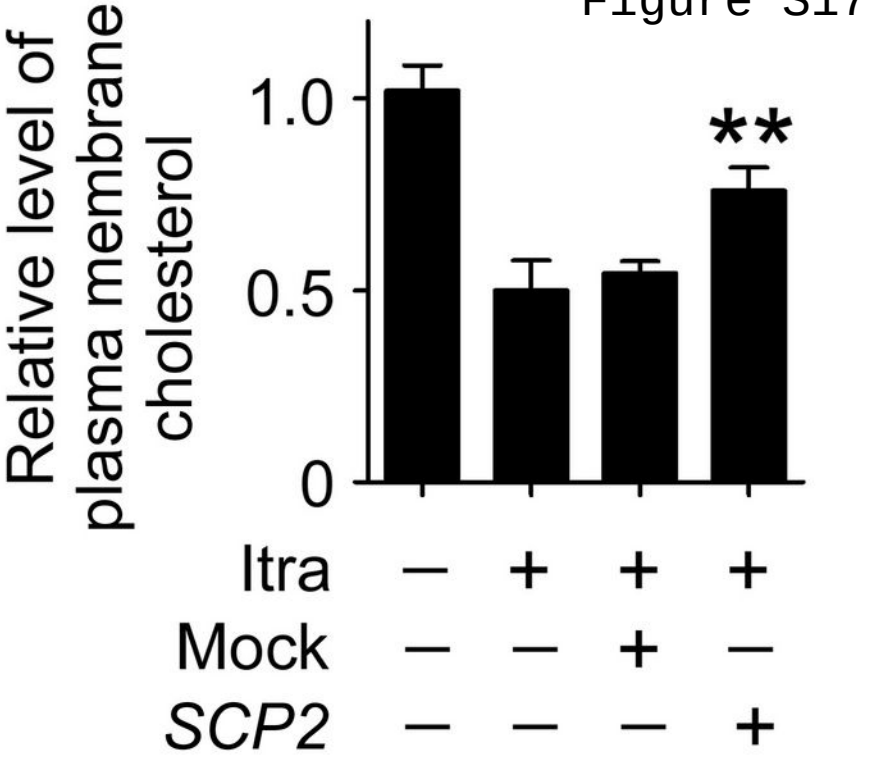
Relative level of plasma membrane cholesterol
1.0
0.5
0
**
Itra — + + +
Mock — — + —
SCP2 — — — +

Figure S18

A

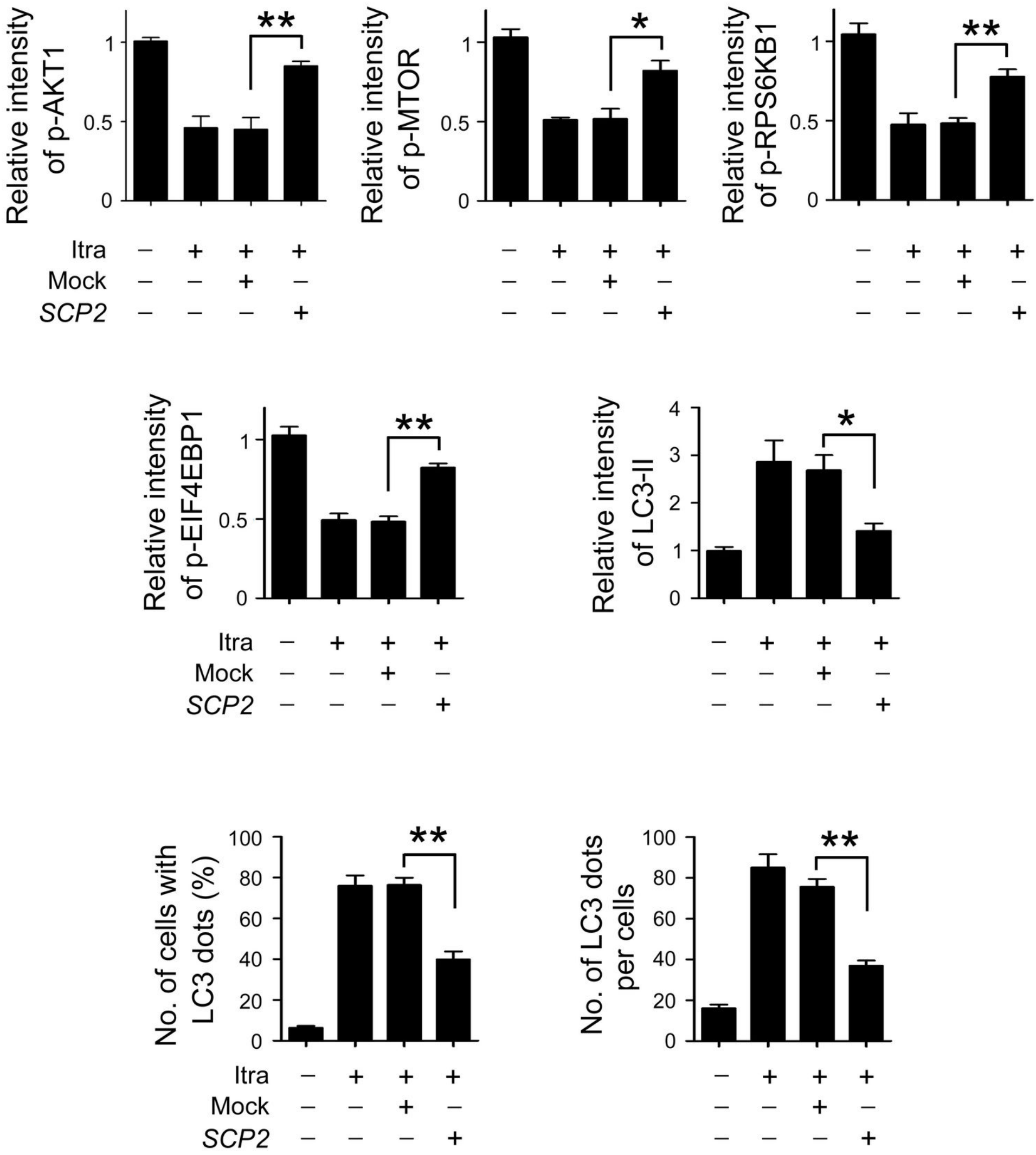

B

Figure S1. Itraconazole induces G1/S arrest in glioblastoma cell lines. U87 or C6 Cells were treated with DMSO or 5 μM itraconazole for 36 h, cell cycle was examined by flow cytometry. The data are representative of 5 independent experiments.

Figure S2. Itraconazole does not induce apoptosis in glioblastoma cell lines cells. U87 or C6 cells were treated with DMSO, 2 or 5 μM itraconazole for 36 h. (**A**) Cell apoptosis was examined by flow cytometry. Dot plot display of ANXA5 FITC-fluorescence versus PI fluorescence shown on a logarithmic scale. Early or late apoptotic cells were defined as ANXA5-positive and PI-negative cells (lower right quadrant) or ANXA5-positive and PI-positive (upper right quadrant), respectively. The data are representative of 3 independent experiments. (**B**) Cell apoptosis was examined by TUNEL assay. The TUNEL-positive cells were counted from at least 100 random fields. The data are representative of 3 independent experiments. ns, not significant; Itra, itraconazole.

Figure S3. Itraconazole induces formation of LC3 puncta. (**A**) U87 cells were transfected with a pEGFP-LC3 plasmid. After 36 h, cells were treated with DMSO or the indicated concentrations of itraconazole for another 36 h. Formation of EGFP-LC3 puncta was visualized by fluorescence microscopy. Cells were defined as positive if they had 5 or more EGFP-LC3 puncta in the cytoplasm. The percentage of the cells with EGFP-LC3 puncta and the average number of EGFP-LC3 puncta were

analyzed from at least 100 random fields. The data are representative of 3 independent experiments. (**B**) U87 cells were treated with the indicated concentrations of itraconazole for 36 h, and formation of endogenous LC3 puncta was examined via immunofluorescence staining using a fluorescence microscope. Cells were defined as positive if they had 5 or more endogenous LC3 puncta in the cytoplasm. The percentage of the cells with endogenous LC3 puncta and the average number of endogenous LC3 puncta were analyzed from at least 100 random fields. The data are representative of 3 independent experiments. **, $P < 0.01$; ***, $P < 0.01$; Itra, itraconazole.

Figure S4. Itraconazole induces formation of autophagic vacuoles. (**A**) U87 cells were treated with DMSO or 5 μM itraconazole for 36 h, and formation of autophagic vacuoles was examined by TEM analysis. The ultrastructures were analyzed from at least 100 randomly chosen fields. The data are representative of 3 independent experiments. (**B**) C6 cells were treated with DMSO or the indicated concentrations of 5 μM itraconazole for 36 h, and formation of autophagic vacuoles was examined by TEM analysis. The ultrastructures were analyzed from at least 100 randomly chosen fields. The data are representative of 3 independent experiments. **, $P < 0.01$; Itra, itraconazole.

Figure S5. Itraconazole induces the accumulation of LC3-II and the degradation of SQSTM1. (**A**) U87 cells were treated with DMSO or the indicated concentrations of

itraconazole for 12, 24 or 48 h. Lysosomal protease inhibitors (E64d and pepstatin A each at 10 μg/ml) were applied for 3 h at the end of treatment time. The conversion of LC3-I to LC3-II was examined by immunoblot. The data are representative of 3 independent experiments. (**B**) U87 cells were treated with DMSO or the indicated concentrations of itraconazole for 36 h. Lysosomal protease inhibitors (E64d and pepstatin A each at 10 μg/ml) were applied for 3 h at the end of treatment time. The conversion of LC3-I to LC3-II was examined by immunoblot. The data are representative of 3 independent experiments. (**C**) C6 cells were treated with DMSO or the indicated concentrations of itraconazole for 36 h. Lysosomal protease inhibitors (E64d and pepstatin A each at 10 μg/ml) were applied for 3 h at the end of treatment time of itraconazole. Conversion of LC3-I to LC3-II was examined by immunoblot. The data are representative of 3 independent experiments. (**D**) U87 cells were treated with DMSO or the indicated concentrations of itraconazole for 36 h, and expression of SQSTM1 was determined by immunoblot. The data are representative of 3 independent experiments. (**E**) C6 cells were treated with DMSO or the indicated concentrations of itraconazole for 36 h, and expression of SQSTM1 was determined by immunoblot. The data are representative of 3 independent experiments. *, $P < 0.05$; **, $P < 0.01$; Itra, itraconazole; ns, not significant.

Figure S6. Itraconazole promotes the formation of PtdIns3K-BECN1-ATG14 complexes. (**A to C**) U87 cells were treated with DMSO or 5 μM itraconazole for 36 h. Interaction between PtdIns3K and BECN1 (**A**), BCL2 and BECN1 (**B**) or ATG14

and BECN1 (**C**) was examined by coimmunoprecipitation. The data are representative of 3 independent experiments. (**D**) Nude mice with U87 subcutaneous tumor xenografts were treated with hydroxypropyl-cyclodextrin (vehicle, n = 9) or itraconazole 75 mg/kg (n = 9) twice daily by oral gavage for 3 weeks. The conversion of LC3-I to LC3-II in tumor tissues was examined by immunoblot. The relative intensity of LC3-II in vehicle- or itraconazole-treated groups is shown. The data were obtained from 3 independent experiments for each tumor. *, $P < 0.05$; Itra, itraconazole.

Figure S7. Inhibition of autophagy represses the antiproliferative effect of itraconazole. (**A**) U87 cells were transfected with siNC (negative control) or si*ATG5* for 72 h, and expression of ATG5 was examined by immunoblot. The data are representative of 3 independent experiments. (**B**) U87 cells were transfected with siNC or si*ATG5* for 36 h, and then treated with 5 μM itraconazole for another 36 h. Expression of ATG5 was examined by immunoblot. The data are representative of 3 independent experiments. (**C**) U87 cells were transfected with siNC or si*BECN1* for 72 h, and expression of BECN1 was examined by immunoblot. The data are representative of 3 independent experiments. (**D**) U87 cells were transfected with siNC or si*BECN1* for 36 h, and then treated with DMSO or 5 μM itraconazole for another 36 h. Expression of BECN1 was examined by immunoblot. The data are representative of 3 independent experiments. (**E and F**) U87 cells were transfected with siNC, si*ATG5* or si*BECN1* for 36 h, and then treated with 5 μM itraconazole for

another 36 h. Cell proliferation was examined by colony formation assay (**E**) and BrdU incorporation assay (**F**). The data are representative of 3 independent experiments for both colony formation assay and BrdU incorporation assay. *, $P < 0.05$; **, $P < 0.01$; ***, $P < 0.001$; Itra, itraconazole.

Figure S8. Itraconazole induces autophagy through inhibition of the AKT1-MTOR pathway. (**A**) U87 or C6 cells were treated with DMSO or the indicated concentrations of itraconazole for 36 h. Phosphorylation of MAPK1/3, MAPK11/13/14 or MAPK8/9 was examined by immunoblot. Total MAPK1/3, MAPK11/12/14 or MAPK8/9 was used as internal control, respectively. The data are representative of 3 independent experiments. (**B**) U87 cells were transfected with mock vector or ca-*AKT1*. 36 h after transfection, the cells were treated with DMSO or 5 μM itraconazole for another 36 h. Expression of ca-AKT1 and phosphorylation of MTOR (Ser2448), CDKN1A (Thr145) and CDKN1B (Thr198) was examined by immunoblots. ACTB was used as the internal control for ca-*AKT1*. Total MTOR, RPS6KB1 or EIF4EBP1 respectively was used as the internal control. The data are representative of 3 independent experiments. (**C**) U87 cells were transfected with mock vector or ca-*AKT1*. 36 h after transfection, the cells were treated with DMSO or 5 μM itraconazole for another 36 h. Formation of endogenous LC3 puncta were examined by immunofluorescence staining using a fluorescence microscope. Cells were defined as positive if they had 5 or more endogenous LC3 puncta in the cytoplasm. The percentage of the cells with endogenous LC3 puncta and the average

number of endogenous LC3 puncta were analyzed from at least 100 random fields. The data are representative of 3 independent experiments. (**D**) U87 cells were transfected with mock vector, ca-*AKT1*, siNC (negative control) or si*BECN1*. 36 h after transfection, the cells were treated with DMSO or 5 μM itraconazole for another 36 h. Cell cycle was analyzed by flow cytometry. The data are representative of 3 independent experiments. *, $P < 0.05$;**, $P < 0.01$; Itra, itraconazole.

Figure S9. Itraconazole induces the redistribution of cellular cholesterol. (**A**) U87 or C6 cells were treated with DMSO or 5 μM itraconazole for 36 h, and the plasma membrane fraction isolated. The level of GAPDH, ATP1A1 and MT-CO1 in the plasma membrane fraction and whole cell lysate was examined by immunoblot. Equal amounts of protein from the plasma membrane fraction or whole cell lysate were loaded for immunoblot. The data are representative of 3 independent experiments. PM, plasma membrane; WCL, whole cell lysate. (**B**) U87 cells were treated with DMSO or 5 μM itraconazole for 36 h. Cellular cholesterol distribution was determined by filipin staining coupled with CAV1 or PDIA immunofluorescence staining. The data are representative of 3 independent experiments.

Figure S10. MβCD-cholesterol complex replenishes the membrane cholesterol content. (**A**) U87 (left panel) or C6 (right panel) cells were treated with DMSO or itraconazole (5 μM) in the presence or absence of the MβCD-cholesterol complex (containing 1 mg/ml MβCD and 20 μg/ml cholesterol) for 36 h. The plasma

membrane fraction was isolated by sucrose density gradient centrifugation, and the level of cholesterol in the plasma membrane examined using the Cholesterol Assay Kit. The data are representative of 4 independent experiments. (**B**) U87 cells were treated with DMSO or itraconazole (5 μM) in the presence or absence of the MβCD-cholesterol complex (containing 1 mg/ml MβCD and 20 μg/ml cholesterol) or rapamycin (100 nM) for 36 h. Phosphorylation of MTOR (Ser2448), RPS6KB1 (Ser424 and Thr421) and EIF4EBP1 (Ser65 and Thr70), and conversion of LC3-I to LC3-II were examined by immunoblot. Total MTOR, RPS6KB1 or EIF4EBP1 was used as internal control for p-MTOR, p-RPS6KB1 or p-EIF4EBP1, respectively. ACTB was used as the internal control for LC3. The data are representative of 3 independent experiments. *, $P < 0.05$; **, $P < 0.01$; ***, $P < 0.001$; Itra, itraconazole; Ch/MβCD, MβCD-cholesterol complex; Rapa, rapamycin; ns, not significant.

Figure S11. Itraconazole-induced cholesterol redistribution inhibits the AKT1-MTOR pathway in U87 cell line. U87 cells were treated with itraconazole (5 μM) in the presence of MβCD (1 mg/ml), cholesterol (20 μg/ml) or the MβCD-cholesterol complex (containing 1 mg/ml MβCD and 20 μg/ml cholesterol) for 36 h. Phosphorylation of AKT1 (Ser473), MTOR (Ser2448), RPS6KB1 (Ser424 and Thr421) and EIF4EBP1 (Ser65 and Thr70) was examined by immunoblot. Total AKT1, MTOR, RPS6KB1 or EIF4EBP1 was used as internal control for p-AKT1, p-MTOR, p-RPS6KB1 or p-EIF4EBP1, respectively. The data are representative of 3 independent experiments.

Figure S12. Itraconazole-induced cholesterol redistribution inhibits the AKT1-MTOR pathway in C6 cell line. (**A**) C6 cells were treated with DMSO or itraconazole (5 μM) in the presence or absence of MβCD (1 mg/ml), cholesterol (20 μg/ml) and the MβCD-cholesterol complex (containing 1 mg/ml MβCD and 20 μg/ml cholesterol) for 36 h. Phosphorylation of AKT1 (Ser473), MTOR (Ser2448), RPS6KB1 (Ser424 and Thr421) and EIF4EBP1 (Ser65 and Thr70) was examined by immunoblot. Total AKT1, MTOR, RPS6KB1 or EIF4EBP1 was used as internal control for p-AKT1, p-MTOR, p-RPS6KB1 or p-EIF4EBP1, respectively. The data are representative of 3 independent experiments. (**B**) U87 cells were treated with itraconazole (5 μM) for 36 h, washed with PBS, and then incubated with the MβCD-cholesterol complex (containing 2 mg/ml MβCD and 80 μg/ml cholesterol) for 4 h. Phosphorylation of AKT1 (Ser473), MTOR (Ser2448), RPS6KB1 (Ser424 and Thr421) and EIF4EBP1 (Ser65 and Thr70) was examined by immunoblot. Total AKT1, MTOR, RPS6KB1 or EIF4EBP1 was respectively used as internal control. The data are representative of 3 independent experiments. *, $P < 0.05$; **, $P < 0.01$; ***, $P < 0.001$; ns, not significant; Ch/MβCD, MβCD-cholesterol complex; Itra, itraconazole.

Figure S13. Itraconazole induces autophagy via triggering cholesterol redistribution. (**A**) U87 cells were treated with itraconazole (5 μM) in the presence of MβCD (1 mg/ml), cholesterol (20 μg/ml) or the MβCD-cholesterol complex (containing 1 mg/ml MβCD and 20 μg/ml cholesterol) for 36 h. Conversion of LC3-I to LC3-II was examined by immunoblot. ACTB was used as the internal control for LC3. The data

are representative of 3 independent experiments. (**B**) C6 cells were treated with DMSO or itraconazole (5 μM) in the presence or absence of MβCD (1 mg/ml), cholesterol (20 μg/ml) and the MβCD-cholesterol complex (containing 1 mg/ml MβCD and 20 μg/ml cholesterol) for 36 h. Conversion of LC3-I to LC3-II was examined by immunoblot. ACTB was used as the internal control for LC3. The data are representative of 3 independent experiments. (**C**) U87 cells were treated with itraconazole (5 μM) in the presence or absence of the MβCD-cholesterol complex (containing 1 mg/ml MβCD and 20 μg/ml cholesterol) for 36 h. Formation of endogenous LC3 puncta was examined via immunofluorescence staining using a fluorescence microscope. Cells were defined as positive if they had 5 or more endogenous LC3 puncta in the cytoplasm. The percentage of cells with endogenous LC3 puncta and the average number of endogenous LC3 puncta were analyzed from at least 100 random fields. The data are representative of 3 independent experiments. (**D**) U87 cells were treated with DMSO or 5 μM itraconazole for 36 h in the presence or absence of the MβCD-cholesterol complex (containing 1 mg/ml MβCD and 20 μg/ml cholesterol). The formation of autophagic vacuoles was examined by TEM. The ultrastructures of U87 cells were analyzed from at least 100 randomly chosen fields. The data are representative of 3 independent experiments. (**E**) U87 (left panel) or C6 (right panel) cells were treated with the indicated concentrations of U18666A. Cell viability was determined by the MTT assay. The data are representative of 3 independent experiments. *, $P < 0.05$; **; $P < 0.01$; ns, not significant; Ch/MβCD, MβCD-cholesterol complex; Itra, itraconazole.

Figure S14. Proteomic identification of the differentially expressed proteins in itraconazole-treated U87 cells. (**A**) U87 cells were treated with DMSO and 5 μM itraconazole for 36 h. Total protein was extracted, separated on pH 3 to 10 nonlinear IPG strips in the first dimension followed by 12% SDS-PAGE in the second dimension, and visualized by CBB staining. Differentially expressed proteins were defined as statistically significant based on two criteria: 1) intensity changes >2-fold, and 2) observed in at least 3 of the 4 replicates. Gel spots were selected for *in situ* gel digestion and analyzed using ESI-Q-TOF tandem mass spectrometry. Representative paired 2-DE gels are shown. Two representative spots with altered expression are boxed and indicated as S and M. (**B**) Protein cluster map was generated using Cluster software. Proteins upregulated in itraconazole-treated U87 cells are shown in red, and the downregulated proteins are shown in green. The color intensity corresponds to the degree of alteration as indicated by the color strip at the bottom. (**C**) The corresponding protein spots of SCPX (the SCP2 precursor) and STARD3 in the 2-DE gels are boxed and enlarged. The relative intensity of the protein spots was measured and compared using PDQuest software. **, $P < 0.01$.

Figure S15. Itraconazole inhibits *SCP2* transcription. (**A**) C6, U118, LN-229 and A-172 cells were treated with DMSO or 5 μM itraconazole for 36 h, expression of SCP2 and STARD3 was examined by immunoblot. The data are representative of 3 independent experiments. (**B**) U87 or U118 cells were treated with DMSO or 5 μM

itraconazole for 36 h, and expression of *SCP2* was examined by semi-quantitative RT-PCR. ACTB was used as the internal control. The data are representative of 3 independent experiments. (**C**) U87 or U118 cells were treated with DMSO or 5 μM itraconazole for 36 h. 10 μM chloroquine or 10 μM MG-132 was added in the culture for the last 6 h. Expression of SCP2 was examined by immunoblot. ACTB was used as the internal control. The data are representative of 3 independent experiments. CQ, chloroquine. ns, not significant; *, $P < 0.05$; **, $P < 0.01$; ***, $P < 0.001$; Itra, itraconazole.

Figure S16. Loss of SCP2 expression inhibits AKT1/MTOR pathway and induces autophagy. (**A**) U87 cells were transfected with siNC, si*SCP2*-a or si*SCP2*-b. 36 h after transfection, the cells were incubated with fresh medium or medium containing the MβCD-cholesterol complex (containing 1 mg/ml MβCD and 20 μg/ml cholesterol) for another 36 h. Phosphorylation of AKT1 (Ser473), MTOR (Ser2448), RPS6KB1 (Ser424 and Thr421) and EIF4EBP1 (Ser65 and Thr70) and conversion of LC3-I to LC3-II were examined by immunoblot. Total AKT1, MTOR, RPS6KB1 or EIF4EBP1 was used as internal control for p-AKT1, p-MTOR, p-RPS6KB1 or p-EIF4EBP1, respectively. ACTB was used as the internal control for LC3. The data are representative of 3 independent experiments. (**B**) U87 cells were transfected with siNC, si*SCP2*-a or si*SCP2*-b. 36 h after transfection, the cells were incubated with fresh medium or medium containing the MβCD-cholesterol complex (containing 1 mg/ml MβCD and 20 μg/ml cholesterol) for another 36 h. Formation of endogenous

LC3 puncta was examined via immunofluorescence staining using a fluorescence microscope. Cells were defined as positive if they had 5 or more endogenous LC3 puncta in the cytoplasm. The percentage of the cells with endogenous LC3 puncta and the average number of endogenous LC3 puncta were analyzed from at least 100 random fields. The data are representative of 3 independent experiments. *, $P < 0.05$; **, $P < 0.01$; ***, $P < 0.001$; ns, not significant; Ch/MβCD, MβCD-cholesterol complex.

Figure S17. Overexpression of SCP2 increases the plasma cholesterol content in itraconazole-treated cells. U87 cells were transfected with mock plasmid or SCP2 plasmid. 36 h after transfection, the cells were treated with DMSO or 5 μM itraconazole for 36 h. The plasma membrane fraction was isolated by sucrose density gradient centrifugation, and the level of cholesterol in plasma membrane was examined using the Cholesterol Assay Kit. The data are representative of 4 independent experiments. **, $P < 0.01$; Itra, itraconazole.

Figure S18. Overexpression of SCP2 attenuates itraconazole-mediated MTOR inhibition and autophagy activation. U87 cells were transfected with mock vector or a SCP2 expression plasmid. After 36 h, cells were treated with DMSO or 5 μM itraconazole for another 36 h. (**A**) Phosphorylation of AKT1 (Ser473), MTOR (Ser2448), RPS6KB1 (Ser424 and Thr421) and EIF4EBP1 (Ser65 and Thr70) and conversion of LC3-I to LC3-II were examined by immunoblot. Total AKT1, MTOR,

RPS6KB1 or EIF4EBP1 was used as internal control for p-AKT1, p-MTOR, p-RPS6KB1 or p-EIF4EBP1, respectively. ACTB was used as the internal control for LC3. The data are representative of 3 independent experiments. (**B**) Formation of endogenous LC3 puncta was examined via immunofluorescence staining using a fluorescence microscope. Cells were defined as positive if they had 5 or more endogenous LC3 puncta in the cytoplasm. The percentage of the cells with endogenous LC3 puncta and the average number of endogenous LC3 puncta were analyzed from at least 100 random fields. The data are representative of 3 independent experiments. *, $P < 0.05$; **, $P < 0.01$; Itra, itraconazole.

Table S1. Data of 26 proteins identified by ESI-Q-TOF.

Accession No.	Protein description	Gene name	Compute MW/pI[a]	Expression level[b]
P19623	Spermidine synthase	SRM	33824.68 / 5.30	-
O00299	chloride intracellular channel 1	CLIC1	26791.54 / 5.09	-
P08758	Annexin A5	ANXA5	35805.58/ 4.93	-
P11177	Pyruvate dehydrogenase (lipoamide) beta	PDHB	35904.41/ 5.38	+
P22307	Sterol carrier protein 2	SCP2	58993.62/6.44	-
Q07955	Serine/arginine-rich splicing factor 1	SRSF1	27613.39/ 10.37	-
Q15185	Prostaglandin E synthase 3 (cytosolic)	PTGES3	18697.38/4.32	-
Q96C19	EF-hand domain family, member D2	EFHD2	26566.09 / 5.15	-
P08779	Keratin 16	KRT16	51136.63 / 4.98	+
P25789	Proteasome (prosome, macropain) subunit alpha type, 4	PSMA4	29483.81 / 7.58	+
Q14849	StAR-related lipid transfer (START) domain containing 3	STARD3	50502.14/8.53	+
P14625	Heat shock protein 90kDa beta (Grp94), member 1	HSP90B1	90177.99 / 4.73	-
P15531	NME/NM23 nucleoside diphosphate kinase 1	NME1	17017.53 / 5.82	-
P60604	Ubiquitin-conjugating enzyme E2G 2	UBE2G2	18566.31 /4.62	-
P08670	Vimentin	VIM	53520.49/5.05	-
P35914	3-Hydroxymethyl-3-methylglutaryl-CoA	HMGCL	31546.68 /7.48	+

	lyase			
O14950	**Myosin, light chain 12B, regulatory**	**MYL12B**	**19647.97/4.69**	**-**
P33778	**Histone cluster 1, H2bb**	**HIST1H2BB**	**13819.00/10.32**	**-**
P09382	**Lectin, galactoside-binding, soluble, 1**	**LGALS1**	**14584.51 /5.30**	**+**
O75947	**ATP synthase, H+ transporting, mitochondrial Fo complex, subunit d**	**ATP5H**	**18360.02/5.22**	**+**
P62310	**LSM3 homolog, U6 small nuclear RNA associated (S. cerevisiae)**	**LSM3**	**11714.22 /4.58**	**-**
P20674	**Cytochrome c oxidase subunit Va**	**COX5A**	**12501.17 /4.88**	**+**
P07737	**Profilin 1**	**PFN1**	**14923.04 / 8.47**	**-**
P63104	**tyrosine 3-monooxygenase/tryptophan 5-monooxygenase activation protein, zeta**	**YWHAZ**	**27745.10 / 4.73**	**-**
P25705	**ATP synthase, H+ transporting, mitochondrial F1 complex, alpha subunit 1, cardiac muscle**	**ATP5A1**	**55209.32 / 8.28**	**+**
Q99714	**Hydroxysteroid (17-beta) dehydrogenase 10**	**HSD17B10**	**26791.89 /7.87**	**+**

a) Theoretical molecular mass (kDa) and pI from the ExPASy database.

b) Expression level in 2-DE analysis upon itraconazole treatment for 36 h compared with control (+, increase; -,decrease).